Title

Jak1 Integrates Cytokine Sensing to Regulate Hematopoietic Stem Cell Function and Stress Hematopoiesis

Journal

Cell Stem Cell, 21(4)

ISSN

1934-5909

Authors

Kleppe, Maria
Spitzer, Matthew H
Li, Sheng
et al.

Publication Date

2017-10-01

DOI

10.1016/j.stem.2017.08.011

Peer reviewed

HHS Public Access

Author manuscript

Cell Stem Cell. Author manuscript; available in PMC 2018 March 12.

Published in final edited form as:

Cell Stem Cell. 2017 October 05; 21(4): 489–501.e7. doi:10.1016/j.stem.2017.08.011.

Jak1 Integrates Cytokine Sensing to Regulate Hematopoietic Stem Cell Function and Stress Hematopoiesis

Maria Kleppe[1], **Matthew H. Spitzer**[2,3,4,5], **Sheng Li**[6], **Corinne E. Hill**[1], **Lauren Dong**[1], **Efthymia Papalexi**[1], **Sofie De Groote**[1], **Robert L. Bowman**[1], **Matthew Keller**[1], **Priya Koppikar**[1], **Franck T. Rapaport**[1,7], **Julie Teruya-Feldstein**[8], **Jorge Gandara**[9], **Christopher E. Mason**[9], **Garry P. Nolan**[2,3], and **Ross L. Levine**[1,7,10,11,12,*]

[1]Human Oncology and Pathogenesis Program, Memorial Sloan Kettering Cancer Center, New York, NY 10065, USA

[2]Baxter Laboratory in Stem Cell Biology, Department of Microbiology and Immunology, Stanford University, Stanford, CA 94305, USA

[3]Program in Immunology, Stanford University, Stanford, CA 94305, USA

[4]Department of Pathology, Stanford University, Stanford, CA 94305, USA

[5]Department of Microbiology and Immunology, University of California, San Francisco, San Francisco, CA 94143, USA

[6]Department of Neurological Surgery, Weill Cornell Medicine, New York, NY 10065, USA

[7]Center for Hematologic Malignancies, Memorial Sloan Kettering Cancer Center, New York, NY 10065, USA

[8]Department of Pathology, Icahn School of Medicine, Mount Sinai, New York, NY 10029, USA

[9]Institute for Computational Biomedicine and Department of Physiology and Biophysics, Weill Cornell Medical College, New York, NY 10065, USA

[10]Center for Epigenetics Research, Memorial Sloan Kettering Cancer Center, New York, NY 10065, USA

[11]Leukemia Service, Department of Medicine, Memorial Sloan Kettering Cancer Center, New York, NY 10065, USA

SUMMARY

[*]Correspondence: leviner@mskcc.org.
[12]Lead Contact

AUTHOR CONTRIBUTIONS

M. Kleppe and R.L.L. conceived the project. M. Kleppe, M.H.S., P.K., and R.L.L. designed experiments. M. Kleppe, M.H.S., S.L., F.T.R., G.P.N., R.L.B., J.T.-F., and C.E.M. analyzed data. M. Kleppe, M.H.S., L.D., E.P., C.E.H., S.D., M. Keller, and J.G. performed experiments. M. Kleppe and R.L.L. wrote the manuscript with help from M.H.S. and S.L.

SUPPLEMENTAL INFORMATION

Supplemental Information includes seven figures and seven tables and can be found with this article online at http://dx.doi.org/10.1016/j.stem.2017.08.011.

JAK1 is a critical effector of pro-inflammatory cytokine signaling and plays important roles in immune function, while abnormal JAK1 activity has been linked to immunological and neoplastic diseases. Specific functions of JAK1 in the context of hematopoiesis, and specifically within hematopoietic stem cells (HSCs), have not clearly been delineated. Here, we show that conditional Jak1 loss in HSCs reduces their self-renewal and markedly alters lymphoid/myeloid differentiation in vivo. Jak1-deficient HSCs exhibit decreased competitiveness in vivo and are unable to rescue hematopoiesis in the setting of myelo-suppression. They exhibit increased quiescence, an inability to enter the cell cycle in response to hematopoietic stress, and a marked reduction in cytokine sensing, including in response to type I interferons and IL-3. Moreover, Jak1 loss is not fully rescued by expression of a constitutively active Jak2 allele. Together, these data highlight an essential role for Jak1 in HSC homeostasis and stress responses.

In Brief

Selective JAK1 inhibition has emerged as a potential strategy for treating autoimmune and hematological diseases. Levine and colleagues show that Jak1 integrates multiple cytokine signals in normal and malignant HSCs to regulate their self-renewal and quiescence, highlighting further potential therapeutic benefits and risks of Jak1 inhibition.

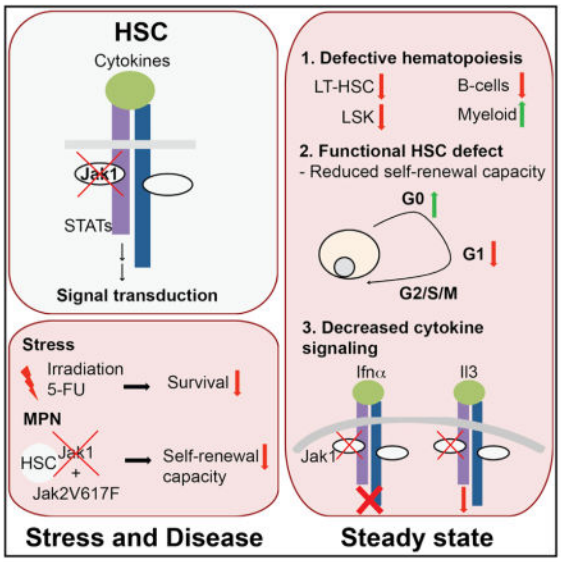

INTRODUCTION

Cytokines play a critical role in hematopoietic lineage choice and self-renewal, and the production of inflammatory cytokines is tightly regulated during normal homeostasis (Baker et al., 2007). Deregulated cytokine production is a characteristic feature of different disease states, including hematologic malignancies and other diseases characterized by chronic inflammation (Brennan and McInnes, 2008). Many pro-inflammatory cytokines are dependent on JAK kinases, including JAK1, to mediate their biological effects (Ghoreschi et al., 2009), and JAK1 activity is required for normal cytokine production leading to a feedback system critical for normal hematopoiesis (Ihle and Kerr, 1995; Murray, 2007).

Moreover, alterations in JAK1 signaling contribute to immunological and hematopoietic diseases (Flex et al., 2008; Jatiani et al., 2010), and selective *JAK1* inhibition has recently emerged as a novel potential strategy for the treatment of autoimmune and hematological diseases (Hsu and Armstrong, 2014; Mascarenhas et al., 2014; O'Shea et al., 2013). However, the function of JAK1 in normal hematopoiesis, including in hematopoietic stem cells (HSCs) has not been delineated.

Complete loss of Jak1 in mice results in embryonic/perinatal lethality (Rodig et al., 1998), precluding studies aimed to elucidate the importance of Jak1 signaling in adult hematopoiesis in vivo, with the exception of limited studies of B and T cell proportions at the time of perinatal lethality. To overcome this limitation, we have developed a mouse model that allows for *conditional deletion of Jak1* in the hematopoietic system. We report here that Jak1 plays a critical role in HSC maintenance, in hematopoietic differentiation and in the response to hematopoietic stress.

RESULTS

Development of a Conditional Jak1 KO Allele

To investigate the physiological role of Jak1 in hematopoiesis, we developed a conditional *Jak1* knockout (KO) allele. The targeting vector is designed to delete exons 3 and 4 by *Cre-loxP* technology resulting in a premature stop codon (Figures 1A and S1A). We intercrossed *Jak1fl/fl* mice to a germline Flp-deleter mouse line to excise the neomycin selection cassette and then to the interferon (IFN)-α-inducible *Mx1-Cre* mice. Treatment of 4- to 6-week-old *Jak1fl/fl;Mx1-Cre*-positive mice with poly(I:C) resulted in undetectable Jak1 protein levels in hematopoietic tissues (Figure 1B), consistent with generation of a KO allele. In line with loss of Jak1 function, we observed decreased Stat3 phosphorylation in peripheral blood cells of *Mx1-Cre*-positive mice (Figure 1C).

Hematopoietic Loss of Jak1 Results in Myeloid Skewing

We analyzed hematopoiesis in *Mx1-Cre*-negative and -positive mice (termed Jak1 KO hereafter) 2–3 months after poly(I:C) injection. Jak1 KO mice were viable and had normal body weight (data not shown). Jak1 KO mice had reduced white blood cell (WBC) counts with an absolute reduction in all hematopoietic cell types (Figures 1D and S1B). Notably, analysis of peripheral blood cells of Jak1 KO mice showed expansion of $CD11b^{+}GR1^{+}$ myeloid cells and a significant reduction in $B220^{+}$ lymphocytes (Figure S1C). By contrast, platelet counts and hematocrit levels were normal in these mice (Figure S1D). Spleen and thymus weights were significantly reduced in Jak1 KO mice (Figures 1E), whereas the total number of bone marrow mononuclear cells showed no significant difference between Jak1 KO mice and littermate controls (Figure S1E).

Defective Hematopoietic Differentiation in Jak1 KO Mice

To better elucidate phenotypic abnormalities in the hematopoietic compartment, we established a surface marker map of the hematopoietic system of Jak1 KO and control mice using mass cytometry (Table S1). We used the SCAFFoLD algorithm (Spitzer et al., 2015) to transform high-dimensional single-cell expression data from Jak1 KO and wild-type mice

into intuitive and interactive maps with population landmark points (Figures 1F and S1F; Table S2). Consistent with a defect in lineage specification, the SCAFFoLD maps revealed that Jak1 KO mice had a marked reduction in the frequency of $B220^+$ cells and an increase in $CD11b^+$ myeloid cells in bone marrow and spleen (Figures 1F, 1G, S1F, S2A, and S2B). Within the $CD11b^+$ population, the percentage of $Ly6C^{hi}Ly6G^-$ monocytes, $Ly6G^+Ly6C^+$ neutrophils, and Siglec-F^+ eosinophils was increased in the absence of Jak1 (Figure 1G). Further, we observed a mild increase in the number of $CD4^+$ and $CD8^+$ T cells in the spleen (data not shown).

In order to better define the effect of Jak1 loss on B cell development, we established a population-specific landscape for $B220^+$ bone marrow cells (Table S2). We clustered $B220^+$ cells from each sample independently, scaled each cluster by frequency, and mapped Jak1 KO and wild-type data together into a force-directed graph (Figures S2C and S2D) (Spitzer et al., 2015). Jak1 KO mice showed near complete loss of $B220^{low}IgM^+IgD^-$ immatureB cells, consistent witha block at anearly stage of B cell development (Figure S2C). This observation was confirmed using flow cytometry (Figures S2E). We observed a 5-fold increase in the relative frequency of $CD19^-PDCA1^+CD11c^+$ plasmacytoid dendritic cells (pDCs) within the $B220^+$ population and a near complete loss of $B220^+CD11c^+NK1.1^+$ natural killer (NK) cells with Jak1 loss, suggesting a key role for Jak1 signaling in innate immune cells (Figures S2C and S2F). Mice transplanted with CD45.2, *Mx1-Cre*-positive bone marrow cells showed a reduction of donor-derived B cells and an increase of donor-derived myeloid cells along with a reduction of the number of peripheral WBC (Figures S2G and S2H).

HSC Defect in Jak1 KO Mice

Cytokines play a critical role in the determination of the different fates of HSCs, and many cytokines activate JAK1to relay extracellular regulatory signals to the nucleus (Baldridge et al., 2010, 2011; Challen et al., 2010; Essers et al., 2009; Mossadegh-Keller et al., 2013; Pronk et al., 2011). This prompted us to investigate whether JAK1 signaling is required for normal HSC function. We observed a significant reduction in the frequency of $lineage^-$ $sca1^+ckit^+$ cells (LSKs), $CD34^-Flk2^-$ long-term HSCs (LT-HSCs), and in $CD34^+Flk2^-$ short-term HSCs (ST-HSCs) in JAK1 KO mice (Figures 2A–2C and S3A). We also observed a reduction in the frequency of LT-HSCs when gating on SLAM family markers (Figures 2D and S3A). In contrast to the reduction of LSKs, we observed an increase of $lineage^-ckit^+sca1^-$ myeloid progenitors (Figure S3B) and in the frequency of common myeloid progenitor (CMP) cells (Figure 2E). Jak1 KO bone marrow cells formed fewer colonies compared to control bone marrow, which was also seen when colony assays were performed in the presence of the JAK1 inhibitor GLPG0634 (Figures 2F–2H). Taken together, these results suggest a role for Jak1 in HSC maintenance.

Marked Functional Defect of Jak1 KO Cells in Bone Marrow Transplantation Assays

We next sought to assess the functional requirement for Jak1 in HSCs by performing competitive bone marrow transplantation assays. We transplanted Jak1 KO or wild-type whole bone marrow cells with equal numbers of CD45.1 whole bone marrow cells into congenic recipient mice (Figure 3A). Flow analysis at 4 weeks post-transplantation showed

3-fold reduced blood chimerism in recipients transplanted with Jak1 KO bone marrow (Figure 3B), with near-complete loss of Jak1 KO cells by 16 weeks consistent with loss of self-renewal (Figures 3B and 3C). The transplantation defect of Jak1 KO cells was not attributable to defects in marrow homing (Figure S4A). Excision of Jak1 after engraftment in recipient mice (Figure 3D) resulted in a significant competitive defect in competitive transplantation assays (Figures 3E and S4B). The reduction in chimerism seen with Jak1 loss was not due to differential myeloid/lymphoid chimerism, as we observed a significant reduction in the proportion of CD45.2 cells in unfractionated spleen and bone marrow 16 weeks after transplantation (Figure 3F). We observed a 3-fold reduction in donor chimerism of LSKs in the bone marrow of Jak1 KO-transplanted mice demonstrating the defect was observed in early stem and progenitor cells (Figure 3G). We observed the same effect on competitive transplantation capacity in Jak1 mice crossed to tamoxifen-inducible *ERT2-Cre* deleter mice, suggesting that this was not due to a poly(I:C) effect on HSCs (Figures 3E, 3F, and S4C). Further, we transplanted CD45.1 wild-type cells into Jak1 KO and control mice and followed the frequency of CD45.1-positive cells in the transplanted recipients over time. We did not observe any difference between the ability of normal hematopoietic cells to reconstitute Jak1 KO or wild-type mice excluding non-hematopoietic contributions to the stem cell phenotype (Figure S4D). Taken together, these data demonstrate a functional defect in self-renewal in Jak1-deficient HSCs.

Jak1 KO Mice Display Increased Mortality after Myelosuppression

We next examined the response of Jak1 KO mice to stress-induced myelosuppression. We first injected Jak1 KO and control mice with a single dose of 5-fluorouracil (5-FU). 5-FU-treated Jak1 KO mice exhibited significantly lower WBCs compared to 5-FU-treated control mice and a reduced WBC rebound from a single hematopoietic stress insult (Figure S4E). These results prompted us to investigate the sensitivity of Jak1 KO cells to repetitive 5-FU treatment, which induces HSC exhaustion. Jak1 KO mice had significantly worse survival when injected with serial doses of 5-FU at 10-day intervals (Figures 3H and S4F). All Jak1 KO mice died within 10 days after administration of the second 5-FU dose, whereas control mice survived the second 5-FU treatment (Figure 3H). In response to radiation-induced myelo-suppression Jak1 KO mice displayed worse survival compared to control mice (Figure 3I). These data suggest that Jak1 KO HSCs are more sensitive to the detrimental effects of hematopoietic stressors.

Loss of Jak1 Causes Increased HSC Quiescence

In response to stress, an increasing subset of HSCs must exit quiescence and enter the cell cycle; previous studies have demonstrated a role for specific cytokines in this process (Baldridge et al., 2011; Zhang and Lodish, 2008). After replenishment of the hematopoietic compartment, most HSCs return to a quiescent state and reestablish a dormant pool of functional stem cells (Wilson et al., 2009). We hypothesized that Jak1 KO HSCs exhibited defective cell-cycle regulation resulting in exhaustion of stem cell function. We measured 5-iodo-2’-deox-yuridine (IdU) incorporation directly in S-phase cells using mass cytometry in order to assess cell-cycle status. We detected a significant reduction of IdU^+ LSKs in Jak1 KO mice and a decrease in the fraction of LSKs in S phase, indicating that Jak1 KO stem cells are less proliferative (Figures 4A and S5A). A significantly larger proportion of Jak1-

deficient LSKs was found to lack expression of the proliferation marker Ki67, consistent with a more quiescent state of Jak1 KO stem/progenitor cells (Figure 4B).

Loss of Jak1 in HSCs Results in Loss of Key Gene Expression Programs, Including IFN-Regulated Gene Programs

To begin to determine the mechanism by which Jak1 regulates normal HSC function, we assessed the impact of Jak1 loss on transcriptional output. We performed RNA-sequencing analysis of $CD150^{+}CD48^{-}$ LT-HSCs isolated from primary wild-type and Jak1 KO mice (Figure S5B). We performed unsupervised hierarchical clustering, which separated the samples into their respective genotypes (Figure 4C). To elucidate Jak1-mediated gene expression changes, we applied a generalized linear model to identify 259 differentially expressed genes of which 85 genes were upregulated (log2-fold change >0) and 175 genes were downregulated (log2-fold change <0) in Jak1 KO LT-HSC compared to control cells (Table S3; Figure S5C). The genes most highly downregulated in Jak1-deleted stem cells included the Jak1 downstream targets Stat1 and Stat2 and multiple members of the IFN regulatory transcription factor family (Figure 4D). These data suggested an important role for Jak1 in mediating Stat1/2 and IFN regulatory transcription factor function at a transcriptional level.

We next performed gene set enrichment analysis (GSEA) (Table S4) (Subramanian et al., 2005). The top ranked gene sets that were suppressed in Jak1 KO HSCs included IFN and inflammatory response signatures (Figure 4E; Table S5). In order to prioritize putative gene sets we next performed a network analysis of the GSEA results using Enrichment Map (Merico et al., 2010). Utilizing this network-based visualization tool, we identified three major clusters related to cell-cycle regulation, inflammatory/IFN response, and hemostasis in the GSEA results (Figure 4F; Table S6). Of note, in addition to canonical IFN signaling pathways, we observed marked downregulation of the E2F and Myc pathways, suggesting Jak1 regulates additional key pathways independent of IFN signaling (Figure S5D; Table S5). We identified 14 known cell-cycle regulators that were transcription-ally downregulated in Jak1-deficient LT-HSCs, including Stat1, Cdk6, and Itgb3 (Figures 4G and S5E). The reduced expression of Cdk6 in Jak1 KO LT-HSCs prompted us to perform CFU assays in the absence or presence of the Cdk4/6 inhibitor PD332991. We observed a significant reduction of the number of colonies compared to DMSO and a reduction in the number of cells per colony (Figures 4H and S5F), suggesting an involvement of Cdk6 in the control of the quiescent state of Jak1-deficient stem cells. These results underscore the dysregulation of the balance between quiescence and cell-cycle entry in Jak1 KO stem cells and, in addition, suggests an underlying defect in IFN signaling pathway output in the absence of Jak1 kinase activity.

Jak1-Deficient Stem and Progenitor Cells Are Resistant to Type I IFN Signaling

IFN-α treatment has been shown to contribute to the exit from HSC dormancy and to drive active cell-cycle entry (Essers et al., 2009; Pietras et al., 2014); however, IFN-α deletion in HSCs has a modest impact on stem cell function. These observations, coupled with our gene expression data, prompted us to test whether Jak1-deficient stem cells have a dense defect in sensing and signaling in response to multiple type I IFNs. We exposed sorted Jak1-deficient

and wild-type LSKs to increasing concentrations of IFN-α or IFN-γ and subsequently assessed the phosphorylation level of Stat1 and Stat5 by flow cytometry and by mass cytometry. As expected, wild-type LSKs showed dose-dependent activation of Stat1 and Stat5 in response to IFN-α and IFN-γ (Figures 5A and S6A). In contrast, Jak1-deficient LSKs showed no change in the phosphorylation status of Stat1 and Stat5 upon IFN-α stimulation and a near-complete loss of the response to IFN-γ stimulation (Figures 5A, S6A, and S6B). Western blot analysis of bulk splenocytes showed that loss of Jak1 leads to decreased sensitivity to IFN-γ stimulation ex vivo (Figure S6C). Further, flow analysis of hematopoietic stem and progenitor cells (HSPCs) from Jak1 KO isolated 6 hr post-poly(I:C) injection showed no increase in Stat1 activation, in contrast to wild-type HSPCs, which showed a signaling response when injected with poly(I:C) (Figure S6D).

Our phenotypic analysis showed that Sca1 expression levels are significantly lower in Jak1-deficient LSKs (Figure S3A). Previous studies have shown that Sca1 expression increases upon IFN-α exposure of LSKs (Essers et al., 2009; Morcos et al., 2017). Consistent with a defective IFN response upon loss of Jak1, Jak1-null hematopoietic cells failed to upregulate Sca1 surface expression in response to IFN-α secretion caused by a single injection of poly(I:C) in vivo (Figure 5B). In wild-type mice, IFNα-induced upregulation of Sca1 is associated with an expansion of the LSK compartment due to an elevated frequency of $Flk2^{-}$ $CD48^{+}$ LSKs ($MPPF^{-}$) and a simultaneous reduction of CMPs (Figure 5C) (Pietras et al., 2014). These changes were not observed in the bone marrow of poly(I:C)-treated Jak1 KO mice. We further found that Jak1-deficient LSKs fail to enter the cell cycle upon poly(I:C) treatment (Figure 5D) (Essers et al., 2009; Pietras et al., 2014). Next, we assessed the effect of genetic deletion of Jak1 on type I IFN-dependent expansion of LSKs ex vivo. Reduced activation of Jak1 resulted in a significant and dose-dependent reduction of the number of LSKs (Figure 5E). Last, we assessed whether Irf7, an important IFN regulatory transcription factor whose expression was markedly reduced in Jak1-deficient LT-HSCs, is a potential downstream mediator of Jak1-mediated stem cell function. Consistent with this hypothesis, *Irf7*-deleted hematopoietic cells show a competitive disadvantage in the setting of in vivo transplantation assays (Figure 5F). Taken together, our data demonstrate Jak1-deficient cells do not respond to type I IFN stimulation, which leads to defects in stem cell phenotype and function.

Jak1 Is Critical for IL-3 Signaling in HSCs

Recent studies have shown that IFN-α activates dormant HSCs in vivo; however, $IFN\text{-}\alpha r^{-/-}$ HSCs do not demonstrate a competitive disadvantage over wild-type cells in transplant assays (Essers et al., 2009). By contrast, Jak1-deficient HSCs are rapidly outcompeted by wild-type cells in competitive transplant assays suggesting an IFN-independent component for Jak1 signaling in HSCs. In order to identify additional signaling pathways that could contribute to the dense phenotype, we tested the response of Jak1-deficient stem cells to a set of hematopoietic cytokines in an ex vivo proliferation assay. Wild-type stem cells expanded ex vivo in response to granulocyte colony-stimulating factor (G-CSF), interleukin-3 (IL-3), IL-6, and type I IFNs, but not IL-2 and IL-7. Likewise, we observed that Jak1-deficient stem cells had an intact proliferative response to G-CSF and IL-6 stimulation. However, we observed a significantly blunted response of Jak1-deficient LSK

cells compared to wild-type cells when cultured in the presence of IL-3 (Figure 6A). Jak1-deficient LSKs showed reduced levels of Stat5 phosphor-ylation in response to IL-3 compared to wild-type cells, but comparable levels of Stat3 and Stat5 activation upon stimulation with G-CSF and IL-6 (Figures 6B, S6E, and S6F), suggesting a critical role of Jak1 for IL-3 signaling in stem cells.

We postulated that the defect in IL-3 signaling in Jak1-deficient stem cells could be correlated with changes in proliferation. To test this, we assessed the single-cell proliferation kinetics of LT-HSCs from Jak1 KO and wild-type mice in the presence and absence of IL-3 and/or IL-6. No significant proliferation was observed in Jak1 KO and wild-type LT-HSCs under basal conditions (Flt3l, Scf) (Figures 6C and 6D). IL-6 induced HSC proliferation in both Jak1-deficient and wild-type cells (Figure 6D). Notably, IL-3 did not show any significant effect on proliferation in Jak1-deficient LT-HSCs, while wild-type cells proliferated in response to IL-3 (Figure 6C). These data suggest that Jak1-defieicent LT-HSCs have an intrinsic defect in IL-3 responsiveness. We next assayed the ability of Jak1-deficient LSKs to form colonies in the presence of IL-3 and observed a 50% reduction in colony numbers (Figure 6E). Consistent with the genetic data, exposure to the Jak1 inhibitor GLPG0634 inhibited the expansion of wild-type cells ex vivo by the addition of IL-3 and IFN-α (Figure 6F). Our data suggest disruption of both IFN-dependent and IFN-independent signaling pathways contribute to the stem cell defect in Jak1 KO mice.

Jak2 Activation Cannot Fully Rescue the Functional Stem Cell Defect of Jak1 KO Cells, Consistent with Non-redundancy among JAK Kinases

We next wanted to assess potential redundancy between different JAK kinases in HSCs. We crossed conditional Jak1 KO mice to *Jak2V617F*-knockin mice (termed Jak2V617F hereafter) to test whether constitutively activated Jak2 could rescue the stem cell defect observed in Jak1 KO mice. We first injected whole bone marrow cells from Jak1 KO, Jak2V617F, Cre-negative control mice, and double transgenic Jak1 KO-Jak2V617F mice (termed J1/J2 hereafter) into congenic recipients. Jak2V617F-transplanted mice developed signs of leukocytosis upon gene deletion, while Jak1 KO-transplanted mice developed leukopenia (Figure 7A). Interestingly, recipient mice transplanted with J1/J2 cells showed WBC counts comparable to control mice (Figure 7A). Myeloid and lymphoid lineage reconstitution was not significantly different between mice transplanted with Jak1 KO cells and Jak1 KO cells with constitutive Jak2 activation (Figure S7A). We next injected the cells into congenic recipient mice along with CD45.1 competitor bone marrow cells (Figure 7B). In line with recent reports, Jak2V617F-expressing cells showed a competitive advantage with increased donor-derived blood chimerism (Mullally et al., 2010). At 12 weeks post-transplantation, we observed a modest rescue of the repopulation capacity of Jak1 KO cells by the presence of the constitutively active *Jak2* allele (Figure 7C). We detected an increase in the proportion of CD45.2 cells in the bone marrow and in the donor chimerism of LSKs of mice transplanted with J1/J2 cells compared to Jak1 KO cells alone (Figures S7B and 7D); however, this did not return to chimerism levels seen in wild-type or in Jak2V617F mutant cells transplanted in vivo.

To further assess the self-renewal Jak1-deficient HSCs with and without Jak2 activation, we harvested bone marrow cells from primary transplant recipient mice and transplanted them into lethally irradiated secondary recipient mice. Jak1 KO cells showed a significant decline in their reconstitution potential in serial transplants relative to Jak1 wild-type cells (Figures 7E and S7C). As previously reported, the phenotype of Jak2V617F-expressing cells was transplantable into secondary and tertiary recipients (Mullally et al., 2010). Notably, loss of Jak1 in these cells resulted in a significant decline in the cells' reconstitution potential in serial transplants relative to Jak2V617F-expressing cells, with near-complete loss of J1J2 cells in tertiary transplants (Figure 7F). Together, our data suggest there is non-redundant signaling between Jak1 and Jak2 in HSCs and that loss of Jak1 signaling attenuates self-renewal in Jak2V617F myeloproliferative neoplasm (MPN) stem cells.

DISCUSSION

Careful regulation of the balance between self-renewal and lineage commitment of HSCs is essential to ensure blood homeostasis, particularly in the setting of acute stressors including myelosuppressive insults and infections (Baldridge et al., 2011; Pietras et al., 2014). Previous studies have delineated a role for specific cytokines in regulating the balance between quiescence and cell-cycle entry, including IFN-α (Essers et al., 2009). However, the role of specific kinases in mediating cytokine signals to maintain this balance in HSCs has not been delineated. Here, we show that Jak1 serves as central conduit for cytokine signaling that is required for HSC function and for stress hematopoiesis.

Previous studies of neonatal *Jak1* deletion mice ($Jak1^{-/-}$) indicated that Jak1 plays a role in neuronal development and survival and in the response to viral infection (Rodig et al., 1998). Notably, fetal liver cells from germline $Jak1^{-/-}$ mice had a markedly attenuated response to lymphopoietic γc receptor cytokines. We show that conditional, somatic loss of Jak1 in the hematopoietic compartment leads to a profound defect in B lymphopoiesis in our Jak1 KO mice, and in loss of $B220^{+}$ NK cells (Blasius et al., 2007; Zitvogel and Housseau, 2012). Moreover, our data suggest there is an important role for Jak1 in mediating humoral and innate immunity and in immunosurveillance. Subsequent studies are needed to delineate the role of Jak1 in specific lymphoid subsets, and to delineate whether Jak1 has a role in normal immune function and in the role of the immune system in responding to neoplastic and infectious insults.

Importantly, here we describe an unexpected role for Jak1 in HSC function. Mass cytometry analysis elucidated a significant defect in LT-HSC and ST-HSC subsets, which was further underscored by the dense defect in competitive repopulating potential and by the increased sensitivity to myelosuppression in the setting of hematopoietic-specific Jak1 loss. Given that JAK1-specific inhibitors are in clinical trials for neoplastic and autoimmune diseases and that the dual JAK1/JAK2 inhibitor ruxolitinib is approved for MPN patients, these data suggest that potent JAK1 inhibition may result in defects in lymphoid function and in HSC function in the setting of myelosuppression. Recent reports have suggested that patients on chronic ruxolitinib therapy may have an increased risk of opportunistic infections (Caocci et al., 2014; Colomba et al., 2012; Goldberg et al., 2013; Wathes et al., 2013; Wysham et al., 2013) and that ruxolitinib therapy in the setting of bone marrow transplantation might

impact engraftment and long-term transplantation outcome (Robin et al., 2013). As such, it will be important to delineate whether these effects are due to JAK1 inhibition and to determine whether selective JAK1 inhibition has similar impact on immune and stem cell function in the human context.

Proper sensing of inflammatory signals, including from type I IFNs and IL-3, under stress conditions is a prerequisite for rapid increases in cycling and differentiation behavior of HSCs during times of stress. Transcriptional and signaling studies demonstrate that Jak1 KO stem cells are insensitive to IFN-α. Of note, previous studies have shown that, while LSKs isolated from IFN-αr KO mice show nearly identical defects in the response to ligand stimulation as Jak1-deficient LSKs, IFN-αr-deficient stem cells have preserved stem cell repopulating potential and function (Essers et al., 2009). These data suggested to us that Jak1-deficient stem cells are insensitive to multiple cytokine stimuli, which collectively are required for stem cell function and homeostasis. Our data highlight a function for IL-3-mediated Jak1 signaling in regulating quiescence/activation state of LT-HSCs and underscores previous studies pointing toward a role of IL-3 as a survival factor in stress hematopoiesis (Hérodin et al., 2003). Overall, our data suggest that Jak1-deficient LT-HSCs have an intrinsic functional defect due to abnormal cytokine responsiveness, which leads over time to stem cell depletion at steady-state and to a dramatic loss of Jak1-deficient LT-HSCs under stress conditions and impaired reconstitution post-myeloablation.

The observation that Jak1-deficient stem cells showed impaired cytokine-sensing ability and reduced stem cell function led us on to investigate whether constitutive Jak2 activation can partially or completely compensate for loss of Jak1 signaling in stem cells. Of note, Jak2 activation was only able to modestly improve the repopulating capacity of Jak1 KO stem cells. Jak2V617F mutant/Jak1-deficient stem cells had reduced stem cell function, including in serial transplantation assays, compared to Jak2V617F mutant stem cells with intact Jak1 function. These studies lead to two important conclusions. First, there is non-redundancy between the different Jak kinases in normal HSC function, suggesting a dynamic interplay between different cytokines and their kinase effectors in mediating normal stem cell function. Second, although Jak1 is not required for the myeloid expansion induced by Jak2V617F, MPN stem cells require Jak1 signaling for function. Subsequent studies in MPN models, and in other malignant contexts, will allow us to elucidate the precise role of Jak1 in malignant stem cells and the potential for Jak1 as a stem-cell target in different cancer contexts.

Taken together, our data highlight a critical role of JAK1 signaling in immune cells and hematopoietic cells. Most importantly, our data underscore the potential benefits and risks associated with JAK1 inhibition as a therapeutic approach in immunological and neoplastic diseases. We expect that subsequent studies will elucidate how key convergent effectors of external signals, such as Jak1, are critical for a broad spectrum of normal and pathologic processes.

STAR+METHODS

KEY RESOURCES TABLE

REAGENT or RESOURCE	SOURCE	IDENTIFIER
Antibodies		
Mouse Anti-Jak1	BD Biosciences	610232
Rabbit Anti-phospho-Stat3	Cell Signaling	9145
Rabbit Anti-Erk1/2	Cell Signaling	4695
CD45.1	Biolegend	110745
CD45.2	Biolegend	109843
Ly6G	Biolegend	127637
IgD	BD Biosciences	553438
CD16/32	BD Biosciences	553141
CD49b	Biolegend	103513
CD11c	BD Biosciences	553799
CD43	BD Biosciences	553268
CD27	Biolegend	124202
CD138	Biolegend	142502
CD34	BD Biosciences	553731
CD41	Biolegend	133919
SiglecF	BD Biosciences	552125
PDCA-1	Imgenex	MAB8660
Ly6C	Biolegend	128039
CD48	Biolegend	103433
CD11b	Biolegend	101249
cKit	Biolegend	105829
CD8	Biolegend	100755
CD4	Biolegend	100561
CD3	BD Biosciences	555273
TCRb	Biolegend	109235
B220	BD Biosciences	103249
NK1.1	Biolegend	108743
CD127	Biolegend	121102
CD105	Biolegend	120401
Sca-1	Biolegend	108135
CD150	eBiosciences	14-1501-82
FcER1a	Biolegend	134321
CD135	eBiosciences	14-1351-82
CD25	Biolegend	101902
F4/80	Biolegend	123143
CD115	Biolegend	135521

REAGENT or RESOURCE	SOURCE	IDENTIFIER
CD71	Biolegend	113802
CD23	Biolegend	101625
CD19	Biolegend	115547
IgM	Biolegend	406527
CD44	BD Biosciences	553131
CD90	Biolegend	105202
MHC II	Biolegend	107637
Ter119	Biolegend	116241
REAGENT or RESOURCE	SOURCE	IDENTIFIER
CD45	Biolegend	103141
pStat3	BD Biosciences	612357
pStat5	Fluidigm	3150005A
pErk1/2	Cell Signaling	4370BF
pStat1	Fluidigm	3153005A
pAkt	Biolegend	649001
p-P38	Cell Signaling	4511BF
Caspase 3	Cell Signaling	9664BF
Ki67	eBiosciences	14-5698-82
PE anti-mouse CD150 (SLAM)	eBiosciences	12-1502-82
BV605 anti-mouse CD150 (SLAM)	Biolegend	115927
PerCP-Cy5.5 anti-mouse CD48	Biolegend	103422
FITC anti-mouse CD48	Biolegend	103403
APC anti-mouse CD135	Biolegend	135309
Alexa Fluor 700 anti-mouse CD34	eBiosciences	56-0341-82
FITC anti-mouse CD34	eBiosciences	11-0341-85
eFluor 450 anti-mouse CD16/32	eBiosciences	56-0161-82
AlexaFluor 700 anti-mouse CD16.32	eBiosciences	56-0161-82
ApC-Cy7 anti-mouse CD11b	Biolegend	101225
PE anti-mouse CD11b	Biolegend	101208
PE-Cy7 anti-mouse B220	Biolegend	103221
APC-Cy7 anti-mouse B220	Biolegend	103224
APC-Cy7 anti-mouse CD19	Biolegend	115530
APC anti-mouse Gr-1	Biolegend	108412
APC-Cy7 anti-mouse Gr-1	Biolegend	108424
APC-Cy7 anti-mouse CD4	Biolegend	100414
Pacific Blue anti-mouse CD8a	Biolegend	100725
Alexa Fluor 488 anti-mouse phospho-Stat1	BD Biosciences	612596
Alexa Fluor 488 anti-mouse phospho-Stat3	BD Biosciences	557814
Alexa Fluor 647 anti-mouse phospho-Stat5	BD Biosciences	562076

REAGENT or RESOURCE	SOURCE	IDENTIFIER
APC-Cy7 anti-mouse CD3	Biolegend	100222
APC-Cy7 anti-mouse NK1.1	Biolegend	108723
APC-Cy7 anti-mouse Ter119	Biolegend	116223
PE anti-mouse cKIT/CD117	Biolegend	105808
APC anti-mouse cKIT/CD117	Biolegend	105812
PE-Cy7 anti-mouse Sca-1	Biolegend	108114
FITC anti-mouse Ki67	eBiosciences	11-5698-82
APC anti-mouse CD45.1	Biolegend	110714
APC anti-mouse CD45.2	Biolegend	109813
PE anti-mouse CD45.1	Biolegend	110707
PE anti-mouse CD45.2	Biolegend	109805
Alexa Fluor 700 anti-mouse CD45.1	Biolegend	110723
Alexa Fluor 700 PE anti-mouse CD45.2	Biolegend	109821
FITC anti-mouse CD45.1	Biolegend	110705
FITC anti-mouse CD45.2	Biolegend	109806
Chemicals, Peptides, and Recombinant Proteins		
5-Fluouracil	Sigma	F6627
GLPG0634	Selleckchem	S7605
$^{191/193}$Ir DNA Intercalator	DVS	201192B
REAGENT or RESOURCE	SOURCE	IDENTIFIER
TRIzol LS Reagent	Fisher	15596018
Methanol	Fisher	A454-4
16% Paraformaldehyde	Elecon Microscope Solution	15710
16% Formaldehyde	Fisher	28906
Tamoxifen	Toronto Research Chemicals	T006000
PD332991	Selleckchem	S1116
Poly(I)-Poly(C)	Amershem	27-4732-01
RPMI Medium 1640	MSKCC Media Core	-
Fetal Bovine Serum	MSKCC Media Core	-
Pen/Strep (100x)	Thermo Fisher Scientific	15140122
MethoCult GF M3434	StemCell Technologies	03434
MethoCult M3231	StemCell Technologies	03231
Recombinant mouse Il3	Peprotech	213-13
Recombinant mouse Il6	Peprotech	216-16
Recombinant mouse Scf	Peprotech	250-03
Recombinant mouse Flt3l	Peprotech	250-31L
Recombinant mouse Ifnα	R&D Systems	12100-1
Recombinant mouse Ifnβ	Peprotech	300-02BC
Recombinant mouse Ifnγ	Peprotech	315-05

REAGENT or RESOURCE	SOURCE	IDENTIFIER
Recombinant human Il2	Peprotech	200-02
Recombinant human Il7	Peprotech	200-07
Recombinant mouse G-Csf	Peprotech	250-05
Critical Commercial Assays		
Fix&Perm Cell Fixation Kit	Thermo Fisher Scientific	GAS004
Gentra Puregene Kit	QIAGEN	158667
TruSeq RNA Library Kit v2	illumina	RS-122-2001
Deposited Data		
RNA-seq	This paper	GEO: GSE85745
Experimental Models: Organisms/Strains		
Jak2V617F	(Mullally et al., 2010)	N/A
R26CreER	The Jackson Laboratory	004847
Jak1	This paper	N/A
B6.Cg-Tg(Mx1-cre)1Cgn/J	The Jackson Laboratory	003556
B6.SJL-*Ptprc*^{a}/BoyAiTac	Taconic	4007
C57BL/6J	The Jackson Laboratory	000664
Oligonucleotides		
see Table S7	N/A	N/A
Software and Algorithms		
SCAFFoLD	https://github.com/nolanlab/scaffold/	N/A
PRISM (version 6)	GraphPad Software	N/A
FCSConcat	Cytobank	N/A
Gephi	https://gephi.org/	N/A
FlowJo (version 9.8.2)	https://www.flowjo.com/	N/A
R (version 3.3.3)	https://cran.r-project.org/	N/A
STAR aligner (version 2.3.0e)	https://github.com/alexdobin/STAR	N/A
GSEA (version 2-2.1.0)	http://software.broadinstitute.org/gsea/index.jsp	N/A
Enrichment Map	http://www.baderlab.org/Software/EnrichmentMap	N/A

CONTACT FOR REAGENT AND RESOURCE SHARING

Further information and requests for resources and reagents should be directed to and will be fulfilled by the Lead Contact, Ross Levine (leviner@mskcc.org).

EXPERIMENTAL MODEL AND SUBJECT DETAILS

Jak1 knock-out mouse model—An 11.98 kb region used to construct the targeting vector was first subcloned from a positively identified C57BL/6 BAC clone (RP23:16H4) using a homologous recombination-based technique. The region was designed such that the long homology arm extends 6.28 kb 5′ to the single LoxP site. The short homology arm extends 2.62 kb 3′ to the LoxP/FRT-flanked Neo cassette. The single LoxP site is inserted upstream of exon 3 in intron 2–3, and the LoxP/FRT-flanked Neo cassette is inserted

downstream of exon 4 in intron 4–5 (target region: 3.08 kb). The targeting vector was confirmed by restriction analysis after each modification step, and by sequencing using primers designed to read from the selection cassette into the 3′ end of the target region and the 5′ end of the SA. The BAC was sub cloned into a ~2.45 kb pSP72 (Promega) backbone vector containing an ampicillin selection cassette for re-transformation of the construct prior to electroporation. A pGK-gb2 LoxP/FRT-flanked Neomycin cassette was inserted into the gene. The targeting construct was linearized using NotI prior to electroporation into ES cells. The total size of the targeting construct is 16.22 kb. Targeted iTL IC1 (C57BL/6N) embryonic stem cells were microinjected into BALB/c blastocysts. Resulting chimeras with a high percentage black coat color were mated to wild-type C57BL/6N mice to generate F1 heterozygous offspring. Tail DNA was analyzed by PCR from pups with black coat color to detect presence of the distal LoxP site using the F1 and R1 primers. Tail DNA samples from LoxP positive mice were then amplified with primers F2 and R2 to confirm SA integration. 5–6 week-old homozygous Jak1 floxed mice were injected with poly(I:C) or tamoxifen to induce gene deletion. Deletion was confirmed 2 weeks later and mice were used for experiments 1–3 months after confirmed deletion. Males and females were used for experiments.

Other animals—Female CD45.1 (B6.SJL-*Ptprc*^{a}/BoyAiTac) mice were purchased from Taconic and were used for competitive and non-competitive transplantation experiments. Female wild-type C57BL/6J were purchased from JAX and used in non-competitive transplant experiments using R26Cre-ER-derived bone marrow. All purchased recipient mice were used at 8–10 weeks. Transgenic heterozygous Jak2V617F knock-in mice (C57BL/6J) were kindly provided by Ann Mullally (DFCI). Mx1-Cre and R26-ER-Cre were purchased from JAX and used for timed mating to generate first offsprings. Healthy animals with an intact immune system were used for all experiments. All animals were drug and test naive and not involved in previous procedures. All mice were housed in the animal facility at Memorial Sloan Kettering Cancer Center in accordance with NIH Guidelines for the Care and Use of Laboratory Animals. Animals were maintained on a 12hr light-dark cycle with access to water and standard chow ad libitum. MSKCC animal care staff conducted routine husbandry procedures and provided daily care and monitoring of all animals housed in MSKCC's animal facilities. Experimental animals were closely monitored by laboratory staff for signs of disease or morbidity, failure to thrive, weight loss > 10% total body weight, open skin lesions, bleeding, infection, or fatigue. Mice developing any of the above complications were sacrificed immediately. All animal experiments were performed with the approval of the Institutional Animal Care and Use Committee of MSKCC.

METHODS DETAILS

Mass cytometry

Antibodies: Antibodies, metals, and manufacturers are listed in Table S1. Antibody staining was performed using two panels. Primary antibody transition metal-conjugates were either purchased (Fluidigm) or conjugated using 100-μg antibody lots combined with the MaxPAR antibody conjugation kit (Fluidigm) according to the manufacturer's instructions.

Sample preparation: Single cell suspensions of BM cells and splenocytes from Jak1 KO and wt mice were prepared 4–8 weeks after poly(I:C) treatment. For stimulation experiments, cells were either stimulated with Ifnα (100U/ml, R&D Systems) or Ifnγ (10ng/ml, Peprotech) for 15 min at 37°C. Unstimulated cells were used as control. IdU was added to the cells at a final concentration of 10μM for 15 min. Cells were then fixed by adding paraformaldehyde (PFA, Electron Microscopy Sciences) directly to the cells at a final concentration of 1.6% and incubated for 10 min at room temperature (RT). Fixed cells were washed twice and stored at −80°C until further processing.

Antibody staining

Barcoding and antibody staining: Prior to antibody staining, mass tag cellular barcoding of prepared samples was performed by incubating cells with distinct combinations of isotopically-purified palladium ions chelated by isothiocyanobenzyl-EDTA in 0.02% saponin in PBS as previously described (Behbehani et al., 2014; Zunder et al., 2015). After two washes with cell staining media (CSM: PBS + 0.5% BSA + 0.02% NaN_3), barcoded samples were pooled together and washed once more with CSM. Barcoded cells were first stained with metal-conjugated CD16.32 antibody and then incubated with a surface marker antibody cocktail (Table S1). For stimulation experiments, surface stained cells were washed twice, and then surface antibodies were fixed by incubation with 1.5% PFA (15 min, RT). Cells were pelleted by centrifugation, permeabilized by adding 4°C methanol slowly to pre-chilled cells and incubated for 10 min at 4°C. Permeabilized cells were washed to remove remaining methanol and then incubated with intracellular antibodies for 30 min at RT. For all experiments, after completion of staining cells were washed twice with staining media and then stained with $^{191/193}$Ir DNA Intercalator (DVS Sciences) diluted in PBS with 1.6% PFA overnight at 4°C.

Mass cytometry: Washed cells were diluted in ddH20 containing bead standards to approximately 10^6 cells/ml. Approximately 0.3–0.5x10^6 cell events were collected for each sample on a CyTOF mass cytometer (DVS Sciences) at an even rate of 300–400 events/second.

Data normalization and de-barcoding: Bead standard data normalization was performed using the CyTOF bead-based normalization software in MATLAB (Finck et al., 2013) and available at https://github.com/nolanlab/bead-normalization. Cells were de-barcoded into their respective conditions using single-cell debarcoding software in MATLAB (Zunder et al., 2015) available at https://github.com/nolanlab/single-cell-debarcoder.

SCAFFoLD maps: To generate SCAFFoLD maps, all datasets for each genotype were combined in a single file using the FCSConcat software by Cytobank (https://support.cytobank.org/hc/en-us/articles/206336147-FCS-fileconcatenation-tool). Each sample was clustered independently into 200 clusters using the *clara* algorithm, and SCAFFoLD maps were generated using the publicly available R package available at github.com/nolanlab/scaffold (Spitzer et al., 2015). Briefly, landmark cell populations were manually identified in the data by gating. A graph was constructed from the data from wild-type mice by first connecting together the nodes representing the manually gated landmark populations

and then connecting to them the nodes representing the cell clusters. Each node is associated with a vector containing the median marker values of the cells in the cluster (blue nodes) or gated populations (red nodes). Edge weights were defined as the cosine similarity between these vectors. Edges of low weight were filtered out, using values of 0.8 for the initial subgraph of landmark nodes and 0.7 for the complete graph as previously determined (Spitzer et al., 2015). The graph was then laid out using an in-house R implementation of the ForceAtlas2 algorithm from the graph visualization software Gephi (Jacomy et al., 2014). To overlay the additional samples on the wild-type map, the position and identity of the landmark nodes was fixed and the clusters of each sample were connected to the landmark nodes as described above. Once again the graphs were laid out using ForceAtlas2 but this time only the blue nodes were allowed to move.

Unsupervised force-directed graphs: The gated cell populations for each tissue were clustered independently using clara in R. The clusters for all the tissues were combined in a single graph with edge weights defined as the cosine similarity between the vectors of median marker values of each cluster. All the pairwise distances were calculated and for each node only the 10 edges of highest weight were retained. The graph was then laid out using the ForceAtlas2 algorithm in Gephi (Jacomy et al., 2014). Visual aesthetics were applied in Gephi by scaling the size of clusters proportional to the frequency of cells from that sample falling into each cluster and by coloring each cluster according to its sample of origin or median expression value for each marker of interest.

Phospho-flow and cell cycle analysis—For phospho-flow analysis, sorted LSKs from experimental mice (*Mx1-Cre* or *ERT2-Cre*) were stimulated with increasing concentrations of Ifnα, Ifnγ, Il3, Il6, or G-Csf for 15 min at 37°C, fixed with formaldehyde, and permeabilized by adding cold 100% methanol slowly to pre-chilled cells, while vortexing. Cells were then stained for 30 min at RT in the dark with phospho-specific antibodies or isotype controls. For cell cycle analysis, BM cells were first surface stained to identify LSKs followed by mild fixation and permeabilization of cells using the FIX & PERM Cell Fixation and Cell Permeabilization Kit (Thermo Fisher Scientific) following the manufacturer's recommendations. Ki67-FITC (eBiosciences) was added to the Medium B prior to permeabilization of the cells. DAPI was used as counterstain. Cell cycle analysis under homeostasis was performed at least 4 weeks post completion of poly(I:C) injections.

Ex vivo proliferation assays—Whole bone marrow cells of experimental mice were seeded out at a concentration of 5.10^6/ml with or without cytokines in triplicate. Cytokines were used at the following concentrations: Il3 (10ng/ml), G-Csf (10ng/ml), Il6 (20ng/ml), Il2 (10ng/ml), Il7 (10ng/ml), Infα (50U/ml), and Ifnγ (1ng/ml). 48 hr later, cells were harvested and surface stained to identify LSK cells. In addition, for each well, cell numbers were recorded to calculate total number of LSKs per well. All experiments were performed at least two to three times. To test the effect of pharmacological Jak1 inhibition on ex vivo proliferation of LSKs in the absence or presence of cytokines, whole BM cells from wt mice were seeded out as described above with or without indicated cytokines in the presence or absence of Jak1 inhibitor GLPG0634 at a concentration of 500nM.

Transplantation experiments—For non-competitive transplants, 10^6 whole BM cells of CD45.2 *experimental* mice were transplanted via tail vein injection into CD45.1 congenic wt recipients. For the reverse experiment, 10^6 whole BM cells of CD45.1 wild-type cells were transplanted via tail vein injection into lethally irradiated CD45.2 experimental mice. For competitive transplants, 0.5×10^6 whole BM cells of CD45.2 *experimental* mice were mixed with equal numbers of CD45.1 wt competitor BM and transplanted via tail vein injection into CD45.1 congenic wt recipients. The transplanting ratio was determined prior to transplantation by flow cytometry. Chimerism and lineage composition was measured by FACS in PB at week 0, 4, 8, 12, and 16 after transplant (excision prior to transplantation) or poly(I:C) injection of recipient mice (excision post transplantation, Figures 3A and 3D). Additionally, for each bleeding, PB counts were measured on a blood analyzer. Total chimerism and chimerism in the stem/progenitor compartment in target organs was evaluated at 16 weeks via animal sacrifice and FACS analysis.

Colony formation unit assays—Whole BM cells of experimental mice were seeded at a density of 10000 cells/replicate into cytokine-supplemented methylcellulose medium (STEMCELL Technologies). Colonies propagated in culture were scored at day 10. To test the effect of pharmacological Jak1 or Cdk6 inhibition, whole BM cells from wt mice were plated with varying concentrations of GLPG0634 or PD332991 (Selleckchem). DMSO was added to control wells. All experiments were performed in triplicate and performed at least three times. Sorted LSKs from Jak1 KO and wt mice (*ERT2-Cre*) were seeded at a density of 500 cells/replicate into cytokine-free methylcellulose medium (STEMCELL Technologies) supplemented with 10 ng/ml Il3 and the number of colonies were scored at day 10. Total cell numbers/well were also recorded to assess the number of cells/colony.

5-FU- and radiation-induced myelosuppression—Mice received one intraperitoneal (i.p.) injection of 5-FU at a dose of 150mg/kg of body weight at 2–3 month after confirmed excision. Blood was collected at day 0 prior to 5-FU injection and again at days 6, 12, and 18. Blood cell counts were measured using the Pro-Cyte Dx Hematology Analyzer (Idexx). For serial 5-FU challenges, mice were injected with serial doses of 150mg/kg of body weight at 10 day intervals and survival of the mice was monitored. To assess radiation-induced myelosuppression, lethally irradiated female CD45.1 mice were transplanted with CD45.2 cells from floxed Jak1 mice crossed to the *ERT2-Cre* deleter line. Upon engraftment, mice received two doses of tamoxifen (i.p.) and excision was confirmed two weeks later (excision efficiency ~80%). Recipient mice transplanted with Cre- or Cre+ cells received a lethal radiation dose of 900 cGy and survival of the mice was monitored. Experiments were performed at least 8 weeks after excision was confirmed.

In vivo poly(I:C) challenge—Jak1 KO and control mice received four i.p. injections of poly(I:C) every other day at a dose of 20mg/kg of body weight at 4–6 weeks after confirmed excision. Mice were sacrificed 24 hr after administration of the final injection and BM cells were analyzed using flow cytometry. Gating strategies used in this study to identify different immature stem and progenitor cell populations in the BM were adopted from (Pietras et al., 2014). For in vivo signaling studies, Jak1 KO and control mice were injected with one dose of poly(I:C) and sacrificed 6 hr later for analysis. Upon isolation of the bone marrow, cells

were kept in the presence of phosphatase inhibitors to preserve the phosphorylation signal. Cells were stained with surface markers to identify hematopoietic stem and progenitor cells (Lin-cKit+) and subsequently processed as described above (see phospho-flow).

Single cell analysis—LT-HSCs (LSK-CD150+CD48-) from experimental mice were directly sorted into Terasaki microassay plates (60 wells, Greiner) containing basal (Scf: 100ng/ml, Flt3l: 2ng/ml), basal plus Il3 (0.2ng/ml) or basal plus Il6 (10ng/ml) supplemented media (RPMI+20% FBS+P/S). Microwells containing a cell at the time of plating were tracked manually by light microscopy. At each time point, the number of total cells per well was counted and normalized to the number of microwells analyzed.

RNA sequencing analysis—Trizol LS was used for RNA extraction of sorted LT-HSCs per manufacturer's recommendation. RNA sequencing libraries were prepared in two batches using TruSeq RNA-Seq by polyA enrichment and sequenced on HiSeq2000 (Illumina) using a 50 bp paired-end approach per manufacturer's recommendations. Alignment was performed using the STAR aligner (version 2.3.0e) (Dobin et al., 2013) and mouse genome mm10 as reference. Aligned results were annotated using the Refseq gene model and featureCounts program from the Subread package (Liao et al., 2014). The significance of Differentially Expressed Genes was determined using DESeq2 Wald significance test (Love et al., 2014). The design matrix includes the latent variables detected by sva to control for any possible batch differences (Leek et al., 2012). For multiple hypothesis testing, the significance cutoff to optimize the independent filtering was 0.05 (Benjamini–Hochberg). GSEA version 2-2.1.0 (http://software.broadinstitute.org/gsea) and msigdb gene sets version 5.0 (n = 10348) were used to determine the sets of genes that are statistically different between two groups using the GSEA Preranked mode (Mootha et al., 2003; Subramanian et al., 2005). To visualize enriched pathways, we used Enrichment Map (Isserlin et al., 2014; Merico et al., 2010). GSEA output files were given to the Enrichment Map app with the following cutoff parameters to build the map: p value < 0.001, q-value < 0.002 and overlap similarity coefficient > 0.5. Nodes in the Enrichment Map represent a set of genes and their connections the set of genes that two nodes have in common. The edge thickness is proportional to the overlap of two gene sets. The node colors map enrichment significance: blue/downregulated, red/upregulated.

Experimental Design—No specific methods were used for randomization and investigators were not blinded to the identity of samples. No statistical methods were utilized to determine sample size. The experiments described in this study were designed to use the minimum number of animals required. Each experiment was performed at least in duplicate to ensure reproducibility. Mice showing gene excision lower than 70% or for which excision could not be confirmed were excluded from the analysis.

QUANTIFICATION AND STATISTICAL ANALYSIS

Blood count analysis and organ weights of primary wild-type and Jak1 KO mice were recorded from at least 10 mice per genotype as indicated in figure legends. For mass cytometry analysis, a total of three independent experiments were performed with 5–7 animals per group. All colony formation assays shown in this study were performed in

triplicate in three independent experiments. For competitive transplantation experiments, 5 recipient mice were used for each donor. Data shown from *Mx1-Cre* and *ERT2-Cre* were confirmed in two independent experiments. Serial 5-FU challenge experiments were performed once with *Mx1-Cre* and confirmed in an independent experiment with mice crossed to the *ERT2-Cre* line. Cell cycle experiments under baseline condition and after poly(I:C) challenge were performed twice with a total of 4–5 mice per group. LT-HSCs isolated from 6 mice per group were analyzed by RNA-sequencing. Phospho-flow analysis of LSKs from JAK1 KO and wild-type mice was performed 3 times with a total of 6 mice/group. For ex vivo proliferation assays, the bone marrow from two JAK1 KO or wild-type mice were combined and the assay was performed in duplicate. Two independent experiments were performed in order to assess the single cell cytokine cell division kinetic of LT-HSCs and for each experiment ~30 LT-HSCs sorted from 1–2 mice were followed over time. The number of animals, cells, and experimental replication can be found in the respective figure legend. The Student's t test (unpaired, two-tailed) was used to compare the mean of two groups. Normality tests were used to test the assumption of normal distribution. For samples with significantly different variances Welch's correct was applied. Data were analyzed and plotted using GraphPad Prism 6 software. Graphs represent mean values ± SEM. Kaplan-Meier survival analysis and longrank test was used to compare survival outcomes between two groups. Two-way ANOVA was used to compare differences between the single cell kinetics of JAK1 KO and wild-type cells in response to different cytokines over time.

DATA AND SOFTWARE AVAILABILITY

The GEO accession number for data generated for this paper is GEO: GSE85745. The dataset contains the 2 batches (n = 3/group, total of 12 samples) of RNA-sequencing data shown in Figure 4.

Supplementary Material

Refer to Web version on PubMed Central for supplementary material.

Acknowledgments

The authors thank members of the Levine and Nolan laboratories for helpful comments and discussion. This work was supported by NCI R35-CA197594-01A1 and NCI CA173636 to R.L.L.; K99 HL122503-01A1 to M. Kleppe; NIH F31 CA189331 to M.H.S.; NIH R01 CA196657, U19 AI057229, U19 AI100627, R33 CA183654, R01 HL120724, DOD grants OC110674 and 11491122, Bill and Melinda Gates Foundation grant OPP1113682, NIAID Bio-informatics Support Contract HHSN272201200028C, and FDA grant 30 HHSF223201210194C BAA-12-00118 to G.P.N. S.L. is supported by grants from the Ty Louis Campbell Foundation and the WorldQuant Foundation. Technical services provided by the MSKCC Core Facilities were supported in part by MSKCC Support Grant/Core Grant P30 CA008748. R.L.L. is a Leukemia and Lymphoma Society Scholar. M. Kleppe is a fellow of the American Society of Hematology and was previously supported by fellowships from the Leukemia and Lymphoma Society and the European Molecular Biology Organization. G.P.N. is a consultant for Fluidigm and the maker of CyTOF. R.L.L. is a consultant for Novartis and is on the Supervisory Board of QIAGEN.

References

Baker SJ, Rane SG, Reddy EP. Hematopoietic cytokine receptor signaling. Oncogene. 2007; 26:6724–6737. [PubMed: 17934481]

Baldridge MT, King KY, Boles NC, Weksberg DC, Goodell MA. Quiescent haematopoietic stem cells are activated by IFN-gamma in response to chronic infection. Nature. 2010; 465:793–797. [PubMed: 20535209]

Baldridge MT, King KY, Goodell MA. Inflammatory signals regulate hematopoietic stem cells. Trends Immunol. 2011; 32:57–65. [PubMed: 21233016]

Behbehani GK, Thom C, Zunder ER, Finck R, Gaudilliere B, Fragiadakis GK, Fantl WJ, Nolan GP. Transient partial permeabilization with saponin enables cellular barcoding prior to surface marker staining. Cytometry A. 2014; 85:1011–1019. [PubMed: 25274027]

Blasius AL, Barchet W, Cella M, Colonna M. Development and function of murine B220+CD11c +NK1.1+ cells identify them as a subset of NK cells. J Exp Med. 2007; 204:2561–2568. [PubMed: 17923504]

Brennan FM, McInnes IB. Evidence that cytokines play a role in rheumatoid arthritis. J Clin Invest. 2008; 118:3537–3545. [PubMed: 18982160]

Caocci G, Murgia F, Podda L, Solinas A, Atzeni S, La Nasa G. Reactivation of hepatitis B virus infection following ruxolitinib treatment in a patient with myelofibrosis. Leukemia. 2014; 28:225–227. [PubMed: 23929216]

Challen GA, Boles NC, Chambers SM, Goodell MA. Distinct hematopoietic stem cell subtypes are differentially regulated by TGF-beta1. Cell Stem Cell. 2010; 6:265–278. [PubMed: 20207229]

Colomba C, Rubino R, Siracusa L, Lalicata F, Trizzino M, Titone L, Tolomeo M. Disseminated tuberculosis in a patient treated with a JAK2 selective inhibitor: A case report. BMC Res Notes. 2012; 5:552. [PubMed: 23039051]

Dobin A, Davis CA, Schlesinger F, Drenkow J, Zaleski C, Jha S, Batut P, Chaisson M, Gingeras TR. STAR: Ultrafast universal RNA-seq aligner. Bioinformatics. 2013; 29:15–21. [PubMed: 23104886]

Essers MA, Offner S, Blanco-Bose WE, Waibler Z, Kalinke U, Duchosal MA, Trumpp A. IFNalpha activates dormant haematopoietic stem cells in vivo. Nature. 2009; 458:904–908. [PubMed: 19212321]

Finck R, Simonds EF, Jager A, Krishnaswamy S, Sachs K, Fantl W, Pe'er D, Nolan GP, Bendall SC. Normalization of mass cytometry data with bead standards. Cytometry A. 2013; 83:483–494. [PubMed: 23512433]

Flex E, Petrangeli V, Stella L, Chiaretti S, Hornakova T, Knoops L, Ariola C, Fodale V, Clappier E, Paoloni F, et al. Somatically acquired JAK1 mutations in adult acute lymphoblastic leukemia. J Exp Med. 2008; 205:751–758. [PubMed: 18362173]

Ghoreschi K, Laurence A, O'Shea JJ. Janus kinases in immune cell signaling. Immunol Rev. 2009; 228:273–287. [PubMed: 19290934]

Goldberg RA, Reichel E, Oshry LJ. Bilateral toxoplasmosis retinitis associated with ruxolitinib. N Engl J Med. 2013; 369:681–683. [PubMed: 23944322]

Hérodin F, Bourin P, Mayol JF, Lataillade JJ, Drouet M. Short-term injection of antiapoptotic cytokine combinations soon after lethal gamma-irradiation promotes survival. Blood. 2003; 101:2609–2616. [PubMed: 12468435]

Hsu L, Armstrong AW. JAK inhibitors: Treatment efficacy and safety profile in patients with psoriasis. J Immunol Res. 2014; 2014:283617. [PubMed: 24883332]

Ihle JN, Kerr IM. Jaks and Stats in signaling by the cytokine receptor superfamily. Trends Genet. 1995; 11:69–74. [PubMed: 7716810]

Isserlin R, Merico D, Voisin V, Bader GD. Enrichment Map—a Cytoscape app to visualize and explore OMICs pathway enrichment results. F1000Res. 2014; 3:141. [PubMed: 25075306]

Jacomy M, Venturini T, Heymann S, Bastian M. ForceAtlas2, a continuous graph layout algorithm for handy network visualization designed for the Gephi software. PLoS ONE. 2014; 9:e98679. [PubMed: 24914678]

Jatiani SS, Baker SJ, Silverman LR, Reddy EP. Jak/STAT pathways in cytokine signaling and myeloproliferative disorders: Approaches for targeted therapies. Genes Cancer. 2010; 1:979–993. [PubMed: 21442038]

Leek JT, Johnson WE, Parker HS, Jaffe AE, Storey JD. The sva package for removing batch effects and other unwanted variation in high-throughput experiments. Bioinformatics. 2012; 28:882–883. [PubMed: 22257669]

Liao Y, Smyth GK, Shi W. featureCounts: An efficient general purpose program for assigning sequence reads to genomic features. Bioinformatics. 2014; 30:923–930. [PubMed: 24227677]

Love MI, Huber W, Anders S. Moderated estimation of fold change and dispersion for RNA-seq data with DESeq2. Genome Biol. 2014; 15:550. [PubMed: 25516281]

Mascarenhas JO, Cross NC, Mesa RA. The future of JAK inhibition in myelofibrosis and beyond. Blood Rev. 2014; 28:189–196. [PubMed: 25043171]

Merico D, Isserlin R, Stueker O, Emili A, Bader GD. Enrichment map: A network-based method for gene-set enrichment visualization and interpretation. PLoS ONE. 2010; 5:e13984. [PubMed: 21085593]

Mootha VK, Lindgren CM, Eriksson KF, Subramanian A, Sihag S, Lehar J, Puigserver P, Carlsson E, Ridderstråle M, Laurila E, et al. PGC-1alpha-responsive genes involved in oxidative phosphorylation are coordinately downregulated in human diabetes. Nat Genet. 2003; 34:267–273. [PubMed: 12808457]

Morcos MNF, Schoedel KB, Hoppe A, Behrendt R, Basak O, Clevers HC, Roers A, Gerbaulet A. SCA-1 expression level identifies quiescent hematopoietic stem and progenitor cells. Stem Cell Reports. 2017; 8:1472–1478. [PubMed: 28506535]

Mossadegh-Keller N, Sarrazin S, Kandalla PK, Espinosa L, Stanley ER, Nutt SL, Moore J, Sieweke MH. M-CSF instructs myeloid lineage fate in single haematopoietic stem cells. Nature. 2013; 497:239–243. [PubMed: 23575636]

Mullally A, Lane SW, Ball B, Megerdichian C, Okabe R, Al-Shahrour F, Paktinat M, Haydu JE, Housman E, Lord AM, et al. Physiological Jak2V617F expression causes a lethal myeloproliferative neoplasm with differential effects on hematopoietic stem and progenitor cells. Cancer Cell. 2010; 17:584–596. [PubMed: 20541703]

Murray PJ. The JAK-STAT signaling pathway: Input and output integration. J Immunol. 2007; 178:2623–2629. [PubMed: 17312100]

O'Shea JJ, Kontzias A, Yamaoka K, Tanaka Y, Laurence A. Janus kinase inhibitors in autoimmune diseases. Ann Rheum Dis. 2013; 72(Suppl 2):ii111–ii115. [PubMed: 23532440]

Pietras EM, Lakshminarasimhan R, Techner JM, Fong S, Flach J, Binnewies M, Passegué E. Re-entry into quiescence protects hematopoietic stem cells from the killing effect of chronic exposure to type I interferons. J Exp Med. 2014; 211:245–262. [PubMed: 24493802]

Pronk CJ, Veiby OP, Bryder D, Jacobsen SE. Tumor necrosis factor restricts hematopoietic stem cell activity in mice: Involvement of two distinct receptors. J Exp Med. 2011; 208:1563–1570. [PubMed: 21768269]

Robin M, Francois S, Huynh A, Cassinat B, Bay JO, Cornillon J, Rolland V, Charbonnier A, Michallet M, Boyer F, et al. Ruxolitinib before allogeneic hematopoietic stem cell transplantation (HSCT) In patients with myelofibrosis: A preliminary descriptive report of the JAK ALLO Study, a phase II trial sponsored by goelams-FIM in collaboration with the Sfgmtc. Blood. 2013; 122:306. [PubMed: 23869074]

Rodig SJ, Meraz MA, White JM, Lampe PA, Riley JK, Arthur CD, King KL, Sheehan KC, Yin L, Pennica D, et al. Disruption of the Jak1 gene demonstrates obligatory and nonredundant roles of the Jaks in cytokine-induced biologic responses. Cell. 1998; 93:373–383. [PubMed: 9590172]

Spitzer MH, Gherardini PF, Fragiadakis GK, Bhattacharya N, Yuan RT, Hotson AN, Finck R, Carmi Y, Zunder ER, Fantl WJ, et al. IMMUNOLOGY. An interactive reference framework for modeling a dynamic immune system. Science. 2015; 349:1259425. [PubMed: 26160952]

Subramanian A, Tamayo P, Mootha VK, Mukherjee S, Ebert BL, Gillette MA, Paulovich A, Pomeroy SL, Golub TR, Lander ES, Mesirov JP. Gene set enrichment analysis: A knowledge-based approach for interpreting genome-wide expression profiles. Proc Natl Acad Sci USA. 2005; 102:15545–15550. [PubMed: 16199517]

Wathes R, Moule S, Milojkovic D. Progressive multifocal leukoencephalopathy associated with ruxolitinib. N Engl J Med. 2013; 369:197–198.

Wilson A, Laurenti E, Trumpp A. Balancing dormant and self-renewing hematopoietic stem cells. Curr Opin Genet Dev. 2009; 19:461–468. [PubMed: 19811902]

Wysham NG, Sullivan DR, Allada G. An opportunistic infection associated with ruxolitinib, a novel janus kinase 1,2 inhibitor. Chest. 2013; 143:1478–1479. [PubMed: 23648912]

Zhang CC, Lodish HF. Cytokines regulating hematopoietic stem cell function. Curr Opin Hematol. 2008; 15:307–311. [PubMed: 18536567]

Zitvogel L, Housseau F. IKDCs or B220+ NK cells are pre-mNK cells. Blood. 2012; 119:4345–4346. [PubMed: 22577157]

Zunder ER, Finck R, Behbehani GK, Amir el-AD, Krishnaswamy S, Gonzalez VD, Lorang CG, Bjornson Z, Spitzer MH, Bodenmiller B, et al. Palladium-based mass tag cell barcoding with a doublet-filtering scheme and single-cell deconvolution algorithm. Nat Protoc. 2015; 10:316–333. [PubMed: 25612231]

Highlights

- Conditional deletion of Jak1 in HSCs alters hematopoietic differentiation
- Jak1 and Jak2 have non-redundant signaling functions in HSC stress response
- Jak1 is a critical mediator of interferon and IL-3 signaling in HSCs
- MPN-like phenotypes induced by Jak2 activation are depending on Jak1 signaling

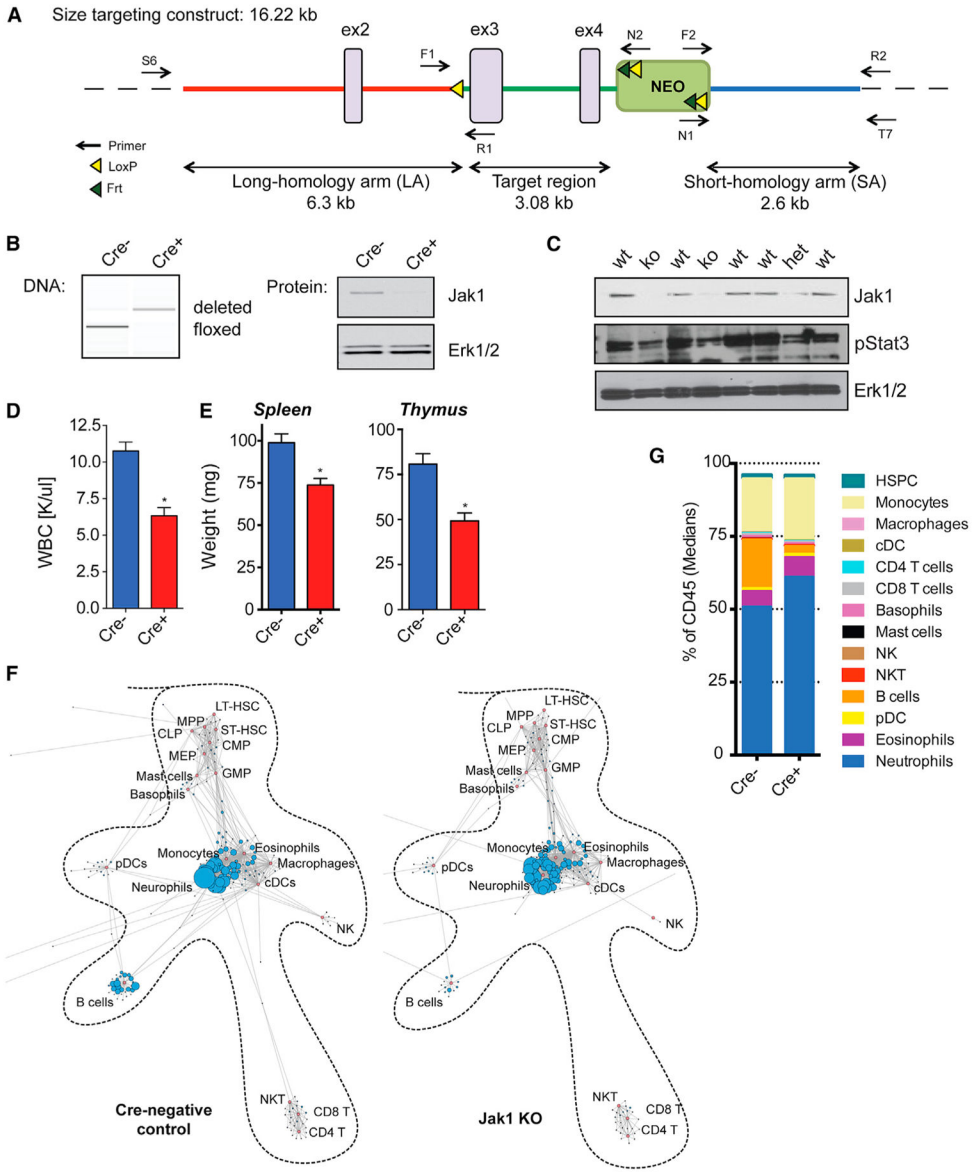

Figure 1. Generation of a Conditional Jak1 Allele and Characterization of Mice with Jak1 Loss in the Hematopoietic System

(A) Design of a conditional targeting vector.

(B) Confirmation of gene and protein deletion in the bone marrow.

(C) Deletion of Jak1 in the hematopoietic system leads to reduced activation of Stat3 in peripheral blood cells. WT, wild-type; het, heterozygous deletion; ko, homozygous deletion.

(D) Jak1 KO mice feature reduced white blood cell (WBC) counts (mean ± SEM). n = 11–13. See also Figure S1.

(E) Jak1 KO mice feature reduced spleen (n = 14) and thymus weights (n = 18). Mean ± SEM. *$p < 0.05$.

(F) Bone marrow SCAFFoLD map for Jak1 KO and *Mx1-Cre*-negative control mice. Red nodes: manually gated landmark populations using Jak1 wild-type as reference sample. Blue nodes: unsupervised cell clusters. n = 5.

(G) Median frequencies of bone marrow cell populations from Jak1 wild-type and KO mice defined by conventional criteria. n = 5.

HSPC, hematopoietic stem and progenitor cell; cDC, conventional dendritic cell; NK, natural killer cell; NKT, natural killer T cell; pDC, plasmacytoid dendritic cell. See also Figure S2.

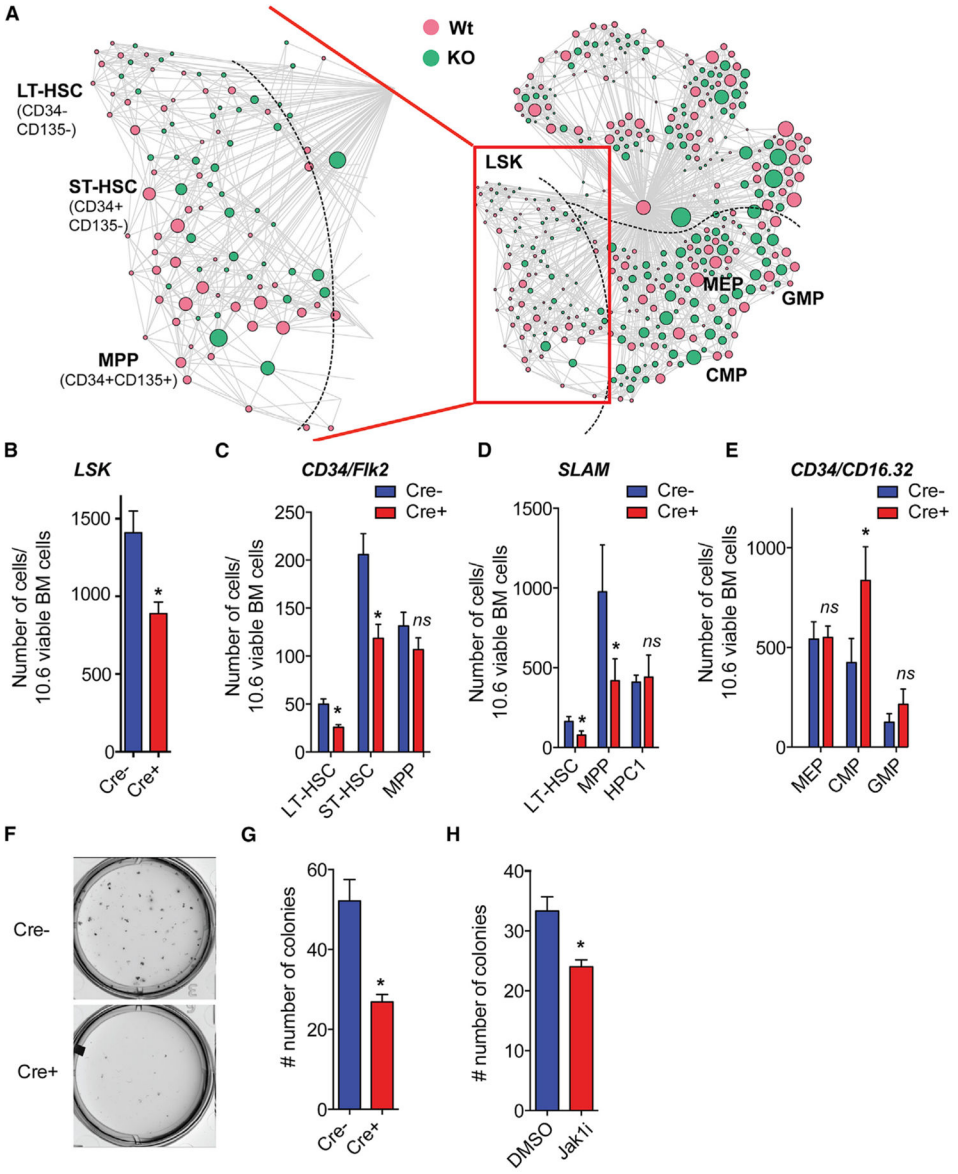

Figure 2. Jak1 Signaling Is Required for Normal HSC Function

(A) Phenotypic landscape of lineage-negative (lin$^-$) cells. Clusters are colored according to genotype (Jak1 wild-type: red, Jak1 KO: green) and sized by the number of cells in each cluster as a percentage of the total number of lin$^-$ cells in the bone marrow. n = 5. LT-HSC, long-term HSC; ST-HSC, short-term HSC; MPP, multipotent progenitors; CMP, common myeloid progenitor; MEP, megakaryocyte-erythroid progenitor; GMP, granulocyte-monocyte progenitor. See also Figure S3.

(B) Manual analysis by traditional criteria confirmed that Jak1 KO mice have a significant reduction of total LSKs in the bone marrow.

(C) Frequency of LT-HSCs (CD34$^-$CD135/Flk2$^-$ LSK) and ST-HSCs (CD34$^+$CD135/Flk2$^-$ LSK) in the bone marrow of Jak1 wild-type (Cre$^-$) and KO mice (Cre$^+$).

(D) Bar graph showing the number of LSK stem cell fractions subdivided according to SLAM markers. n = 11 mice per group.
(E) Relative frequency of progenitor cells in the bone marrow of Jak1 KO (Cre^+) and wild-type mice (Cre^-). n = 6.
(F) Representative image of methylcellulose colony plate 10 days after plating of whole bone marrow from KO and control mice. Images are representative of a total of six mice per group.
(G) Bar graph displaying total number of scored colonies. Data shown are representative of three independent experiments with a total of six mice per group.
(H) Number of colonies formed 10 days after plating of whole bone marrow cells from wild-type mice with or without 500 nM JAK1 inhibitor GLPG0634.
Data are representative of three independent experiments. All data displayed as bar graphs represent mean ± SEM. *$p < 0.05$.

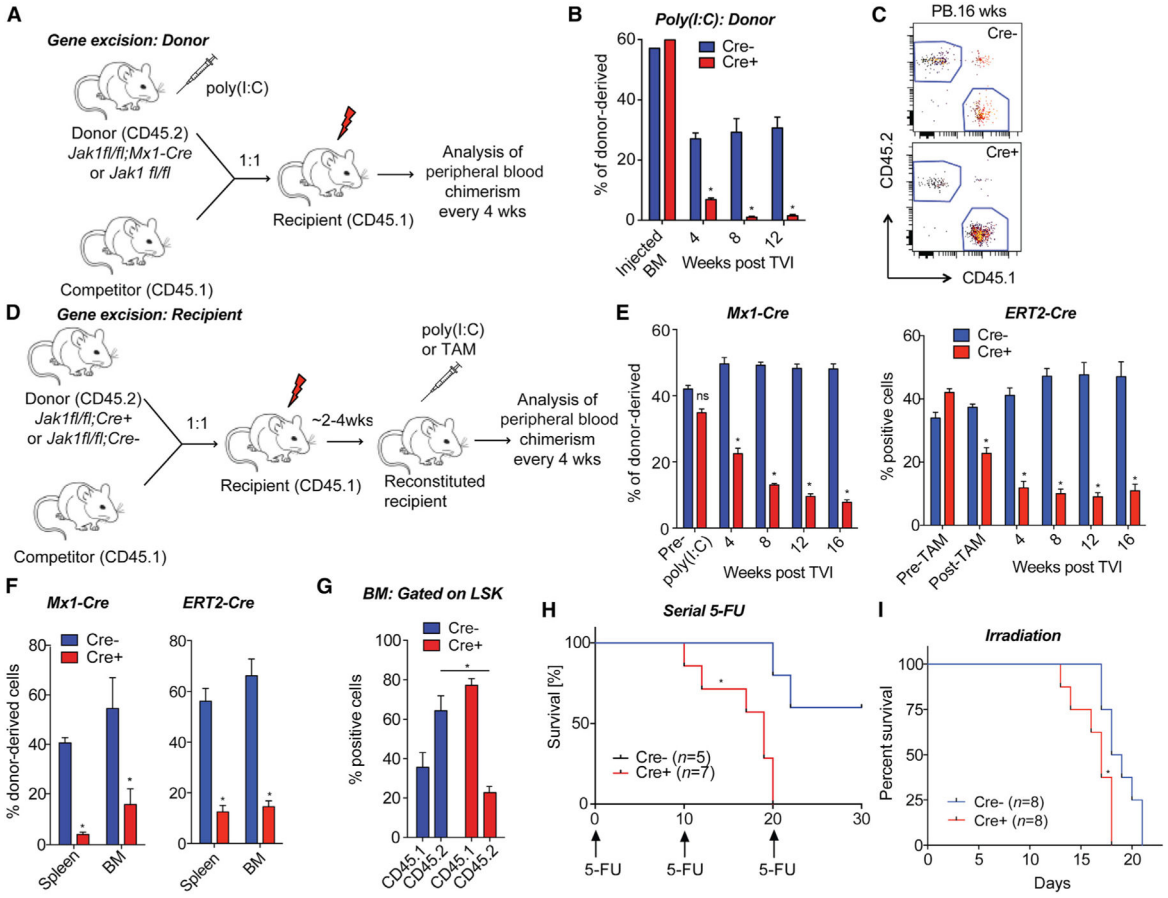

Figure 3. Jak1 Is Required for HSC Stress Responses In Vivo

(A) Schematic diagram showing competitive bone marrow transplant design. Wks, weeks.

(B) Percentage (mean ± SEM) of CD45.1 versus CD45.2 chimerism in the PB of recipients. Excision occurred 3 weeks prior to transplantation. n = 5. *p < 0.05.

(C) Flow cytometric analysis of total chimerism in the periphery 16 weeks post-transplantation. A representative flow plot of a total of five mice per group is shown.

(D) Schematic diagram showing competitive bone marrow transplant design. Wks, weeks.

(E) Percentage (mean ± SEM) of CD45.1 versus CD45.2 chimerism in the PB of recipients at 1, 2, 3, and 4 months after gene deletion in recipient mice. n = 5. *p < 0.05. Data from *Mx1-Cre* and *ERT2-Cre* are shown.

(F) Donor chimerism in the spleen and bone marrow of recipient mice at 16 weeks post-poly(I:C) (*Mx1-Cre*) or tamoxifen (*ERT2-Cre*) injection. n = 5. *p < 0.05.

(G) Donor chimerism within the LSK compartment of recipient bone marrow (*Mx1-Cre*). n = 5. See also Figure S4.

(H) Kaplan-Meier analysis of survival of Jak1 KO (*Mx1-Cre*$^{+}$) and wild-type (*Mx1-Cre*$^{-}$) mice following serial injections of 5-FU (on days 1, 10, and 20). *p < 0.001.

(I) Kaplan-Meier analysis of survival of Jak1 KO (Cre^{+}) and wild-type (Cre^{-}) mice following lethal irradiation (*ERT2-Cre*). *p < 0.05.

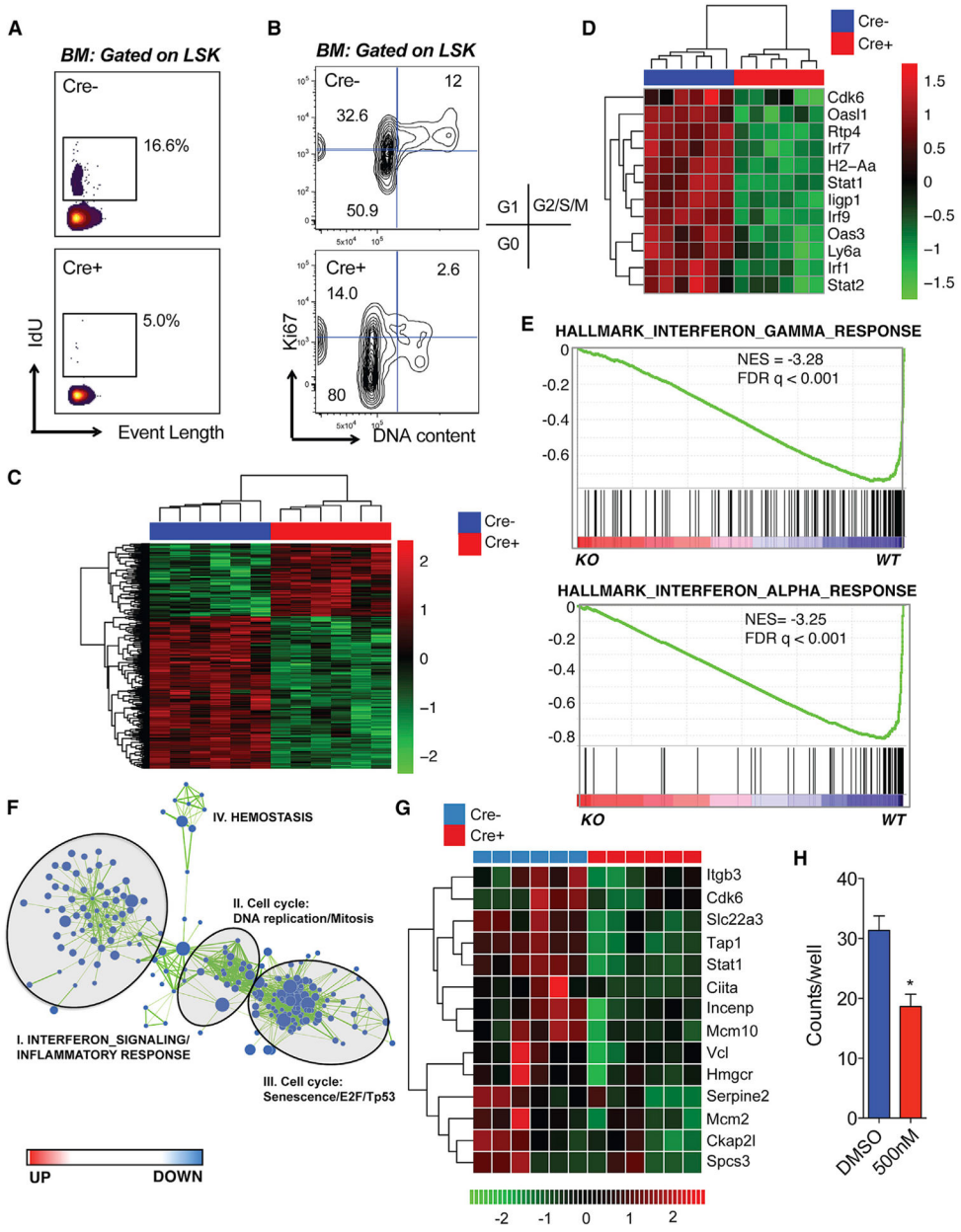

Figure 4. Jak1 KO Stem Cells Display Loss of Interferon-Regulated Gene Programs

(A) Contour plots showing level IdU incorporation in LSKs. Representative data from two independent experiments with n = 5 mice are shown. See also Figure S5.

(B) Representative cell-cycle profiles of LSKs from Jak1 KO (Cre^{+}) and wild-type (Cre^{-}) mice. The percentage of cells in the different cell-cycle stages is presented. n = 4.

(C) Hierarchical clustering of differentially expressed genes.

(D) Heatmap of selected genes identified to be differentially expressed in LT-HSCs of Jak1 KO mice to controls. Data shown are from two independent experiments with a total of six mice per group. See also Figure S5.

(E) GSEA enrichment plots of differentially expressed interferon-related genes associated with loss of Jak1 signaling in LT-HSCs. FDR, false discovery rate; NES, normalized enrichment score.(legend continued on next page)

(F) The networks illustrate the results of the pathway enrichment analysis contrasting Jak1 KO and wild-type HSCs. Each node represents a pathway and the size of each node reflects the number of genes included in the network. The node colors represent the strength and direction of the enrichment.

(G) Heatmap of known cell-cycle regulators identified to be downregulated in LT-HSCs of Jak1 KO mice compared to controls.

(H) Number of colonies formed 10 days after plating of whole bone marrow cells from wild-type mice with or without Cdk4/6 inhibitor PD332991.

Data are representative of three independent experiments. Mean ± SEM. *$p < 0.05$.

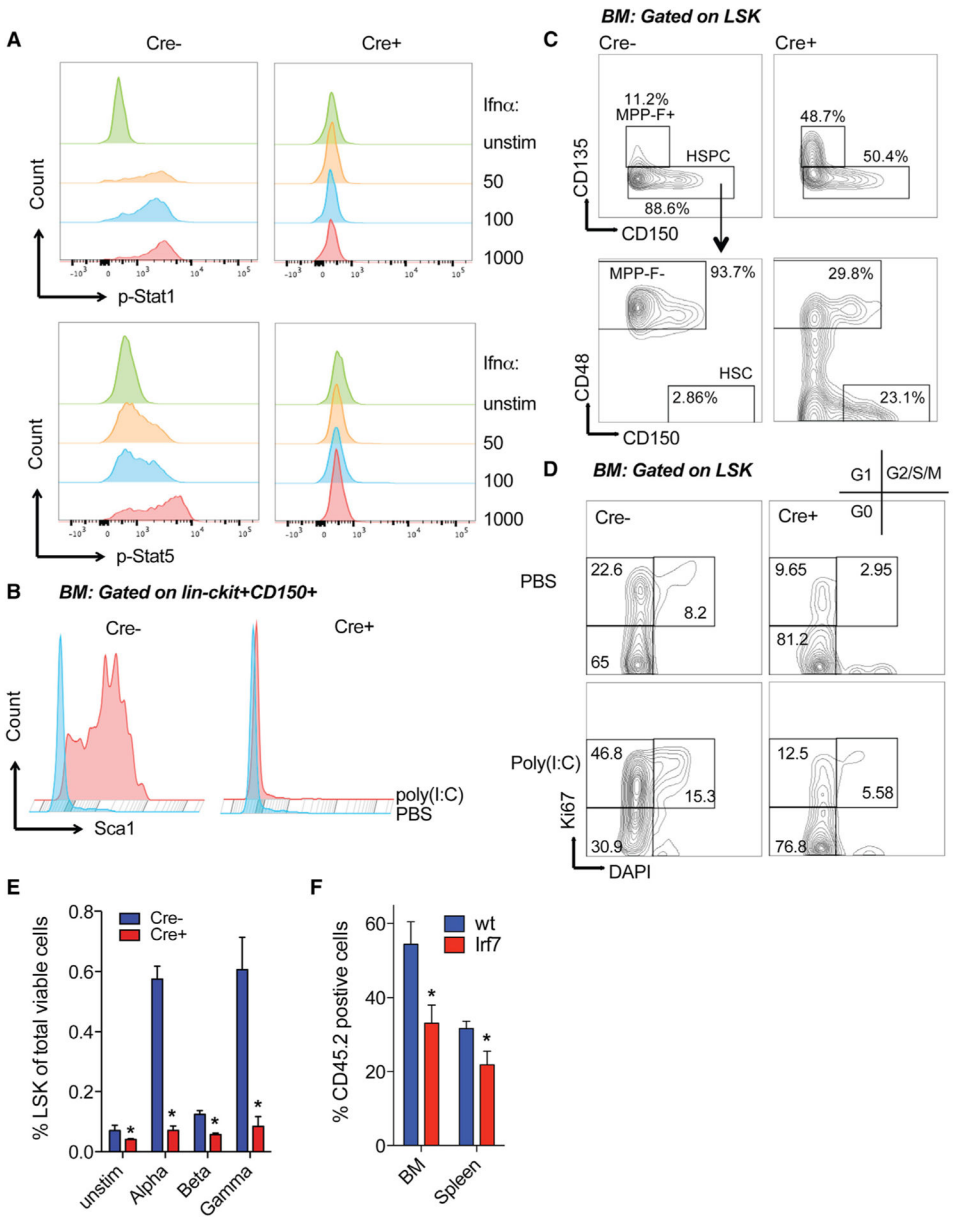

Figure 5. Jak1 KO Cells Are Insensitive to Type I Interferons

(A) Histogram showing the intensity of phospo-Stat1 and phospo-Stat5 versus cell count for LSKs isolated from JAK1 KO and wild-type mice analyzed at baseline (unstim) and in response to increasing IFN-α concentrations. Data are representative of three independent experiments. See also Figure S6.

(B) Flow cytometry histogram showing fluorescence intensity versus cell count for stem cell surface marker Sca1 (Ly6A/E). Representative analysis of viable lin/ckit^{+} bone marrow cells is shown. Analysis was performed 24 hr after injection of the mice with poly(I:C) or PBS (control). n = 2 mice per condition.

(C) Representative cell-cycle profiles of LSKs from poly(I:C) or PBS-treated mice using DAPI and Ki-67. n = 4.

(D) Contour plot showing LSK stem cell fractions subdivided according to CD135 and SLAM markers. MPP-F^{+}, CD135^{+} multipotent progenitors; MPP-F^{-}, CD135^{-}negative multipotent progenitors.

(E) Bar graph depicting the frequency (% of total viable cells) of bone marrow LSKs upon culture ex vivo for 48 hr in the presence or absence of type I and II interferons. Mean ± SEM. Data are representative of two independent experiments and each experiment was performed in triplicate. *$p < 0.05$.

(F) Donor chimerism in the spleen and bone marrow of recipient mice at 16 weeks post-transplantation of whole bone marrow from Irf7 KO or wild-type mice. SEM. *$p < 0.05$ n = 5.

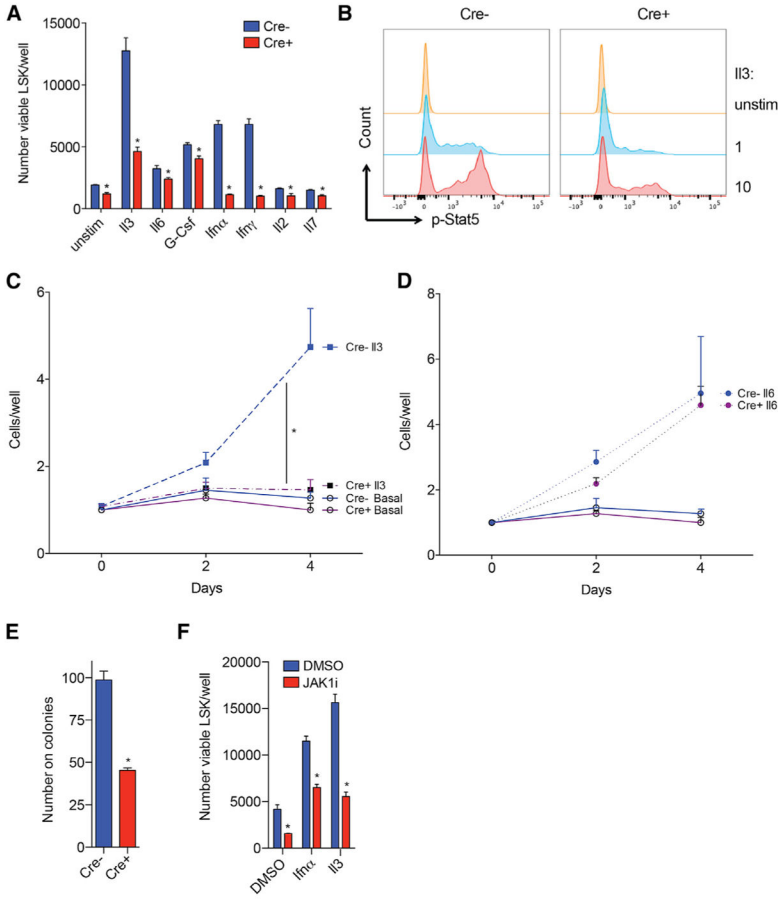

Figure 6. IL-3 Signals through Jak1 in HSCs and Regulates the Balance between Quiescence and Expansion

For a Figure360 author presentation of Figure 6, see the figure legend at https://doi.org/10.1016/j.stem.2017.08.011.

(A) Bar graph depicting the total number of viable LSKs upon culture ex vivo for 48 hr in the presence of indicated cytokines. Mean ± SEM. Data are representative of two independent experiments and each experiment was performed in triplicate. *p < 0.05.

(B) Histogram showing the intensity of phospho-Stat5 versus cell count for LSKs isolated from Jak1 KO and wild-type mice (*ERT2-Cre*) analyzed at baseline (unstim) and in response to increasing IL-3 concentrations. See also Figure S6.

(C and D) Effect of IL-3 (C) and IL-6 (D) on cell proliferation of LT-HSCs from Jak1 KO and wild-type mice. Analysis of proliferation of single cells in microwells was measured as average number of cells in experimental wells at each indicated time point. Basal condition shown in panels (C) and (D) are identical. Data are representative of two independent experiments with about n ~ 30 experimental wells per condition analyzed. Mean ± SEM. *p < 0.001.

(E) Jak1 KO and wild-type LSKs (*ERT2-Cre*) were seeded out in cytokine-free methylcellulose medium supplemented with IL-3 (10 ng/mL). Bar graph displaying total number of scored colonies. *p < 0.05.

(F) Bar graph depicting the total number of viable LSKs upon culture ex vivo for 48 hr in the presence or absence of Jak1 inhibitor (500 nM). Mean ± SEM. Data are representative of two independent experiments, and each experiment was performed in triplicate. *$p < 0.05$.

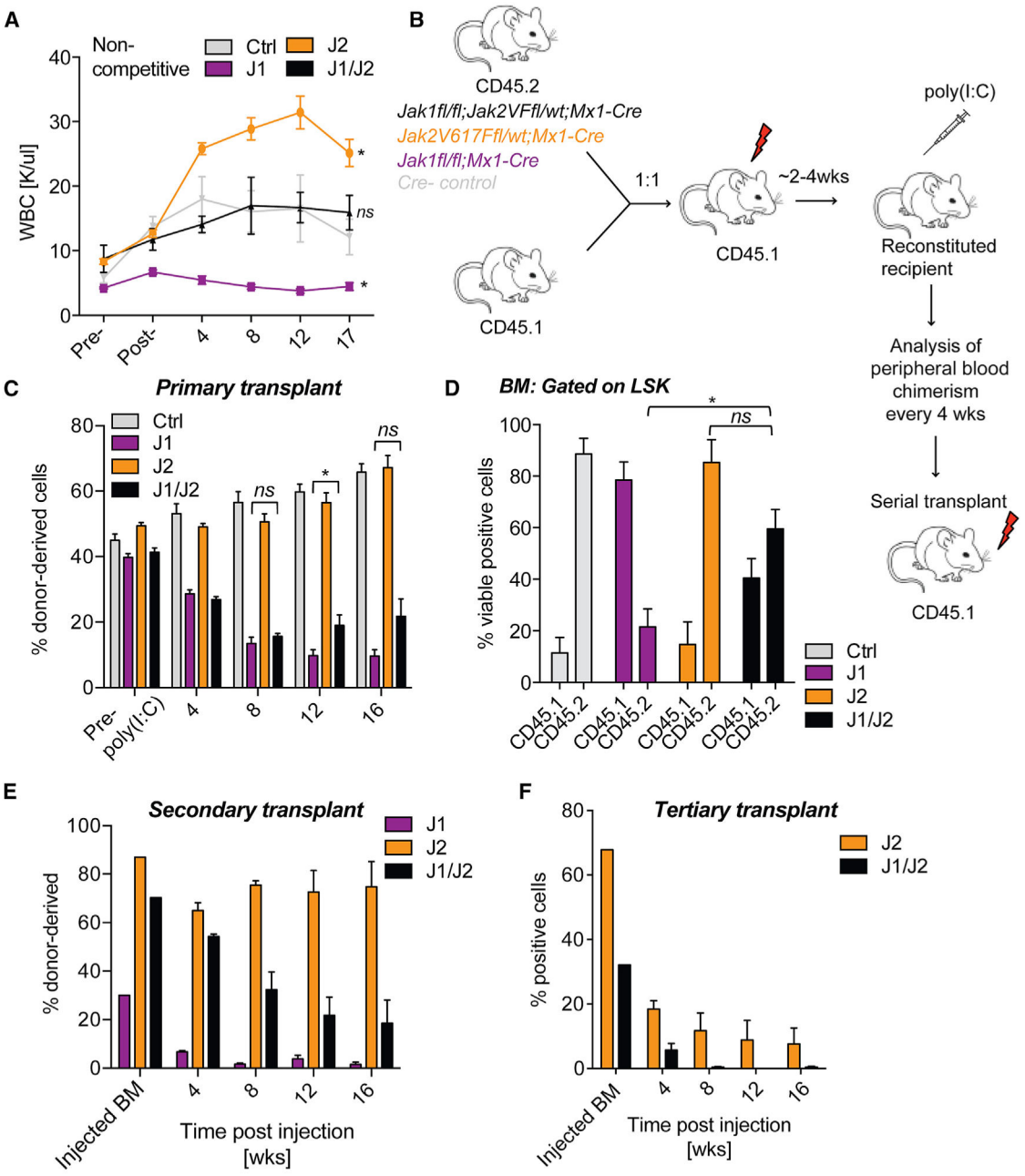

Figure 7. Non-redundant Role of Jak1 Signaling in HSCs

(A) White blood cell (WBC) counts of recipient mice transplanted with whole bone marrow cells. *p < 0.05. n = 5.

(B) Schematic diagram showing competitive bone marrow transplant design.

(C) Percentage (mean ± SEM) of CD45.1 versus CD45.2 chimerism in the PB of recipients at 1, 2, 3, and 4 months after poly(I:C) administration. Pre-poly(I:C) indicates the ratio of CD45.1 to CD45.2 bone marrow cells in recipient mice before gene deletion. n = 5. *p < 0.05.

(D) Donor chimerism within the LSK compartment in the bone marrow of recipient mice at 16 weeks post-poly(I:C) injection. n = 5. *p < 0.05. See also Figure S7.
(E and F) Percentage (mean ± SEM) of donor-derived total CD45.2 cells in the PB of recipient animals. (E) Secondary transplant, (F) tertiary transplants. n = 5 for each genotype. *p < 0.05. ns, not statistical significant. Only genotypes *Jak2V617F* and *Jak1fl/fl,Jak2V617F* were serially transplanted into tertiary recipients.